

Ultrasoft Renormalization in Non-Relativistic QCD

Andre H. Hoang¹ and Iain W. Stewart²

¹*Max-Planck-Institut für Physik ,Föhringer Ring 6, 80805 München, Germany* *

²*Institute for Nuclear Theory, University of Washington, Seattle, WA 98195* †

Abstract

For Non-Relativistic QCD the velocity renormalization group correlates the renormalization scales for ultrasoft, potential and soft degrees of freedom. Here we discuss the renormalization of operators by ultrasoft gluons. We show that renormalization of soft vertices can induce new operators, and also present a procedure for correctly subtracting divergences in mixed potential-ultrasoft graphs. Our results affect the running of the spin-independent potentials in QCD. The change for the NNLL $t\bar{t}$ cross section near threshold is very small, being at the $\lesssim 1\%$ level and essentially independent of the energy. We also discuss implications for analyzing situations where $mv^2 \sim \Lambda_{\text{QCD}}$.

* Electronic address: ahoang@mppmu.mpg.de

† Electronic address: iain@phys.washington.edu

I. INTRODUCTION

The use of effective field theory techniques in non-relativistic fermion-antifermion systems has generated an encouraging record of successes. This framework has applications to describing the dynamics of the bound quarkonium state as well as to heavy quark production and decay (for reviews see Ref. [1]). The formulation of a non-relativistic field theory for fermion-antifermion systems in QED and QCD has gone through several stages of development. In Refs. [2, 3] a method was formulated for separating the short distance physics at the scale m from the long distance physics at the non-relativistic momentum and energy scales, mv and mv^2 . Subsequent work served to clarify the power counting in v , and the description of the low energy degrees of freedom. In particular the relevant low energy degrees of freedom have been classified into potential ($E \sim mv^2$, $\mathbf{p} \sim mv$), soft ($E \sim \mathbf{p} \sim mv$), and ultrasoft ($E \sim \mathbf{p} \sim mv^2$).

It was realized in Ref. [4] that it is necessary to distinguish ultrasoft and soft contributions, and in Ref. [5] that there was a problem with simultaneously power counting the ultrasoft and potential terms in the original NRQCD action. In fact, the ultrasoft gluons destroy the power counting in v unless their Lagrangian is multipole expanded [4, 6]. This can be formulated in an elegant way by introducing more than one type of gluon field in the action [7]. Ref. [8] made the observation that since potential gluons do not propagate they can just as well be integrated out of the theory. In Ref. [9] it was pointed out that in certain situations the matching coefficients can be efficiently computed from what is now known as the hard region of a diagram. This idea was formalized for other momentum regions and more general situations with the advent of the threshold expansion [10], which also emphasized the importance of soft momenta. Finally, the relevance of soft gluons for correctly running α_s in the low energy theory was realized in Ref. [11].

In Refs. [8, 12, 13] the authors went further to suggest that a string of effective theories could be defined by exploiting the hierarchy $m \gg mv \gg mv^2$. We will refer to the theory for scales $mv < \mu < m$ as mNRQCD, and for scales $\mu < mv$ as pNRQCD [8].¹ A correct separation of the mv and mv^2 scales is important since we would like to be confident about what effects can be reliably computed perturbatively, for instance in the case $mv^2 \sim \Lambda_{\text{QCD}} \ll mv$. The mNRQCD–pNRQCD setup appears to rely on being able to treat the energy and momentum scales of the non-relativistic quarks and their corresponding cutoff scales as independent. For static heavy quarks this is the case because the dynamics does not correlate the quark separation $r \sim 1/(mv)$ with energy fluctuations $E \ll mv$.

In Ref. [14] it was pointed out that for dynamic heavy quarks the non-relativistic dispersion relation $E = p^2/(2m)$ couples the energy and momentum scales. The authors therefore proposed matching directly at the scale $\mu = m$ onto a potential-like theory with both soft and ultrasoft degrees of freedom (referred to as vNRQCD). For scales $\mu < m$ the correlation of energy and momenta is accounted for since the ultrasoft and soft scales, μ_U and μ_S , are related, $\mu_U = \mu_S^2/m \equiv mv^2$. The running in the dimensionless velocity parameter from $\nu = 1$ to $\nu \simeq v_0$ of order the velocity of the two particle state, sums logs of both the momenta and the energy at the same time, and is referred to as the “velocity Renormalization Group” (vRGE) [14, 15]. Within dimensional regularization the factors of μ_U^ϵ or μ_S^ϵ multiplying operators in the renormalized effective Lagrangian are uniquely determined from the

¹ Note that we do not use the term NRQCD to refer to a theory for $\mu > mv$. We reserve NRQCD as a generic label for the effective theory(s) which describe $c\bar{c}$, $b\bar{b}$, and $t\bar{t}$ bound state effects.

v power counting in d dimensions [16]. This point is also discussed in Sect. II.

With the vRGE, the running of potentials and currents was worked out in Refs. [14, 15, 17, 18] and applied to $t\bar{t}$ production near threshold in Refs. [19, 20]. The running of the static potential due to ultrasoft effects in the mNRQCD–pNRQCD formalism was computed in Ref. [21]. In Ref. [22] it was shown that the vRGE could be used to predict $\ln \alpha$ contributions in QED bound states, and for positronium the $\alpha^7 \ln^2 \alpha$ hyperfine splitting corrections and $\alpha^3 \ln^2 \alpha$ corrections to decay rates were reproduced, and the $\alpha^8 \ln^3 \alpha$ Lamb shift was predicted. In Ref. [23] it was shown that the correlation of energy and momentum scales is necessary to compute QED corrections involving $\ln^k \alpha$ with $k \geq 2$. More recently, the running of operators in the mNRQCD–pNRQCD framework were computed [24], and the original formalism was modified in Ref. [25] to include the correlation of potential and ultrasoft cutoffs.

The main purpose of this paper is to discuss two aspects of the ultrasoft renormalization of operators for $mv^2 \gg \Lambda_{\text{QCD}}$. We first point out a new set of soft operators which has zero tree-level matching, but is induced by mixing from ultrasoft renormalization of soft time-ordered products. These operators vanish for QED bound states such as Hydrogen or positronium. However they affect the leading logarithmic running of the two spin-independent $1/m^2$ QCD potentials as discussed in Sec. V, and were not included in Ref. [15]. We also compare our results to those in Ref. [24] where analogous operators were included. In Ref. [24] two results were reported, one for scales $mv < \mu < m$ (mNRQCD) and one for $\mu < mv$ (pNRQCD). For the $1/m^2$ potentials we disagree with the mNRQCD results because we find that for dynamic quarks there is no corresponding momentum region we can identify since the renormalization from ultrasoft gluons is always present. For the pNRQCD results we find agreement, however only if we force the mNRQCD–pNRQCD matching scale and the pNRQCD energy cutoffs to always be correlated. We also show that our approach reproduces the $\alpha^6 \ln^2 \alpha$ energy for muonic-Hydrogen with additional massless fermions [26].

Second, we formulate a procedure for correctly subtracting ultrasoft divergences in diagrams containing both ultrasoft and potential loops. Our results for the running of the $1/(m|\mathbf{k}|)$ and $1/\mathbf{k}^2$ QCD potentials differ from Refs. [17, 18, 21, 24], essentially because we find that there is an additional set of operators \mathcal{O}_{ki} , \mathcal{O}_{ci} which must be renormalized. For matrix elements which do not involve additional divergences, the sum of these operators reduce to effective $1/(m|\mathbf{k}|)$ and $1/\mathbf{k}^2$ potentials. For these effective potentials we agree with the $\mu < mv$ pNRQCD results of Ref. [24] (again only if we demand that there is always a correlation between the mNRQCD–pNRQCD matching scale and energy cutoffs). However, our results also apply to matrix elements with additional divergences such as corrections to the $Q\bar{Q}$ current correlators $G(0,0)$, where effective $1/(m|\mathbf{k}|)$ and $1/\mathbf{k}^2$ potentials do not suffice. Numerically the change from the earlier QCD results is quite small, being $\lesssim 1\%$ for the normalization of the $t\bar{t}$ cross section. Our results have implications for the less perturbative situation $mv^2 \sim \Lambda_{\text{QCD}}$ for dynamic quarks. They imply that NRQCD in this situation may be more non-perturbative than sometimes assumed.

In Sec. II we review some of the formalism that we will need. We outline the issues associated with the ultrasoft renormalization of operators in Sect. III as well as our solutions. This is applied to muonic Hydrogen in Sec. IV, the $1/m^2$ QCD potentials in Sec. V, and the effect on the $1/(m|\mathbf{k}|)$ and $1/\mathbf{k}^2$ QCD potentials is taken up in Sec. VI. We discuss the running of the production current in Sec. VII, as well as implications for the scenario where $mv^2 \sim \Lambda_{\text{QCD}}$. In Sec. VIII we discuss results for the production current correlators and give numerical results for the $e^+e^- \rightarrow t\bar{t}$ cross section near threshold. Conclusions are given in

II. FORMALISM

We begin by reviewing some aspects of the NRQCD formalism used here. As a way of motivation it is useful to recall that a properly constructed effective theory should satisfy the following requirements:

1. reproduce the IR divergences of the full theory in its entire region of validity,
2. have a well defined power counting (in v for our case),
3. have no large logs in matching calculations,
4. start with a regulator independent Lagrangian.

The first property ensures that we have included the correct degrees of freedom. The need for the second property is obvious. The third property follows from the first, and the matching will be independent of the IR regulator as long as the same choice is made in the full and effective theories. The fourth property is necessary so that physical predictions are independent of the method used to regulate ultraviolet divergences. In practice we choose dimensional regularization which makes it easy to preserve the symmetries and power counting. For this case the fourth constraint dictates that the action is independent of d when expressed in terms of bare quantities.

The physical system we wish to describe is that of a heavy fermion and antifermion with mass m , and energies $E \sim mv^2$, and momenta $\mathbf{p} \sim mv$ in the c.m. system where $v \ll 1$. The possible degrees of freedom include [2, 3, 4, 5, 6, 7, 8, 9, 10, 11] heavy potential quarks and antiquarks ($\psi_{\mathbf{p}}, \chi_{\mathbf{p}}$), ultrasoft gluons, ghosts, and massless quarks (A^μ, c, φ_{us}), soft gluons, ghosts, and massless quarks (A_q^μ, c_q, φ_q), potential gluons ($A_{\mathbf{p}}^\mu$) and soft heavy quarks and antiquarks (ψ_q^s, χ_q^s). Here, ultrasoft gluons are the gauge partners of momenta $\sim mv^2$, while soft gluons are the partners of momenta $\sim mv$. It is essential that we include both soft and ultrasoft gluons for all scales less than m . Evaluating a generic QCD scattering amplitude in the region of validity of the effective theory gives logarithms

$$\ln(E^2), \quad \ln(\mathbf{p}^2), \quad \ln(\mathbf{k}^2), \quad (1)$$

where E denotes the c.m. energy, \mathbf{p} a quark momentum, and \mathbf{k} the momentum transfer. Both ultrasoft and soft gluons are needed to reproduce the $\ln(E^2)$ and $\ln(\mathbf{k}^2)$ terms. Furthermore, both types of logarithm are needed for all scales below m since both ultrasoft and soft running feed into anomalous dimensions induced by potential loops such as the production current [14] and two-loop renormalization of $1/m^2$ operators in QED [22]. Simultaneously including soft and ultrasoft gluons is also in agreement with the threshold expansion [10] where both soft and ultrasoft regions of energy and momenta are included in calculations in a separated form at scales $\mu \simeq m$. When these degrees of freedom are not treated separately, such as in the mNRQCD-pNRQCD approach for $mv < \mu < m$, the v power counting breaks down, and a $1/m$ expansion with static quarks is used [24]. However, it is argued that a power counting for dynamic quarks exists in pNRQCD for scales $\mu < mv$ [24].

To distinguish the mv and mv^2 scales we made use of a phase redefinition for the potential and soft fields [14]

$$\phi(x) \rightarrow \sum_k e^{-ik \cdot x} \phi_k(x), \quad (2)$$

where k denotes momenta $\sim mv$ and $\partial^\mu \phi_k(x) \sim mv^2 \phi_k(x)$. Since here we will only be interested in cases with perturbative potentials (such as $\Lambda_{\text{QCD}} \ll mv^2$) we simplify the list of degrees of freedom by integrating out potential gluon exchange and soft heavy fermions at the scale m following Ref. [14]. This choice may not be unique, but does allow us to satisfy our effective theory criteria. For instance, in Ref. [16] it was shown that vNRQCD correctly reproduces all the infrared logs in QCD for four-quark Greens functions at one loop in its entire region of validity.

The effective vNRQCD Lagrangian can be separated into ultrasoft, soft, and potential components, $\mathcal{L} = \mathcal{L}_u + \mathcal{L}_s + \mathcal{L}_p$. The presence of two types of gluons immediately brings up the issue of double counting. To avoid double counting the effective theory is constructed such that the ultrasoft gluons reproduce only the physical gluon poles where $k^0 \sim \mathbf{k} \sim mv^2$, while soft gluons give only those with $k^0 \sim \mathbf{k} \sim mv$. The scales for the gluon momenta are influenced by the quark propagators, so the quark-gluon interactions must be constructed in such a way that we will not upset this scaling. In \mathcal{L}_u this is achieved by the multipole expansion of interactions [4, 6], which ensures that ultrasoft gluon momenta are always much smaller than the quark three-momenta. The ultrasoft Lagrangian is [6, 14]

$$\mathcal{L}_u = \sum_{\mathbf{p}} \left\{ \psi_{\mathbf{p}}^\dagger \left[iD^0 - \frac{(\mathbf{p} - i\mathbf{D})^2}{2m} + \frac{\mathbf{p}^4}{8m^3} + \dots \right] \psi_{\mathbf{p}} + (\psi \rightarrow \chi) \right\} - \frac{1}{4} G_u^{\mu\nu} G_{\mu\nu}^u + \dots, \quad (3)$$

where $G_u^{\mu\nu}$ is the ultrasoft field strength. In dimensional regularization the covariant derivative has the form $D^\mu = \partial^\mu + i\mu_U^\epsilon g_u A^\mu$, where $\mu_U = mv^2$ and $g_u = g_u(\mu_U)$ is the renormalized ultrasoft QCD coupling. Note that the covariant derivative only contains the ultrasoft gluon field and that the ultrasoft Lagrangian has the form of the multipole-expanded HQET Lagrangian. For convenience we suppress (throughout this paper) the renormalization Z factors that relate bare and renormalized quantities. The soft Lagrangian has terms [14, 15, 16]

$$\begin{aligned} \mathcal{L}_s = \sum_q \left\{ \bar{\varphi}_q \not{D} \varphi_q - \frac{1}{4} G_s^{\mu\nu} G_{\mu\nu}^s + \bar{c}_q q^2 c_q \right\} \\ - g_s^2 \mu_S^{2\epsilon} \sum_{\mathbf{p}, \mathbf{p}', q, q', \sigma} \left\{ \frac{1}{2} \psi_{\mathbf{p}'}^\dagger [A_{q'}^\mu, A_q^\nu] U_{\mu\nu}^{(\sigma)} \psi_{\mathbf{p}} + \frac{1}{2} \psi_{\mathbf{p}'} \{A_{q'}^\mu, A_q^\nu\} W_{\mu\nu}^{(\sigma)} \psi_{\mathbf{p}} \right. \\ \left. + \psi_{\mathbf{p}'}^\dagger [\bar{c}_{q'}, c_q] Y^{(\sigma)} \psi_{\mathbf{p}} + (\psi_{\mathbf{p}'}^\dagger T^B Z_\mu^{(\sigma)} \psi_{\mathbf{p}}) (\bar{\varphi}_{q'} \gamma^\mu T^B \varphi_q) \right\} + (\psi \rightarrow \chi, T \rightarrow \bar{T}), \end{aligned} \quad (4)$$

where $G_s^{\mu\nu}$ is the soft gluon field strength and $g_s = g_s(\mu_S)$ ($\mu_S = mv$) is the soft QCD coupling. The tensors $U_{\mu\nu}^{(\sigma)}$, $W_{\mu\nu}^{(\sigma)}$, $Z_\mu^{(\sigma)}$, and $Y^{(\sigma)}$ are functions of \mathbf{p}' , \mathbf{p} , q , q' that are generated by integrating out soft heavy quarks and potential gluons. Their explicit form can be found in Ref. [17]. Finally the potential Lagrangian has terms [14, 17]

$$\mathcal{L}_p = -\mu_S^{2\epsilon} V(\mathbf{p}, \mathbf{p}') \psi_{\mathbf{p}'}^\dagger \psi_{\mathbf{p}} \chi_{-\mathbf{p}'}^\dagger \chi_{-\mathbf{p}} + \mu_S^{2\epsilon} F_j^{ABC}(\mathbf{p}, \mathbf{p}') (g_u \mu_U^\epsilon \mathbf{A}_j^C) \left[\psi_{\mathbf{p}'}^\dagger T^A \psi_{\mathbf{p}} \chi_{-\mathbf{p}'}^\dagger \bar{T}^B \chi_{-\mathbf{p}} \right] + \dots, \quad (5)$$

where $\mu_S^{2\epsilon}V$ and $\mu_S^{2\epsilon}F_j^{ABC}$ are functions involving bare Wilson coefficients. In the first term spin and color indices on V and the fermion fields have been suppressed. Matching perturbatively at m and integrating out the potential gluons generates the terms

$$\begin{aligned}
V(\mathbf{p}, \mathbf{p}') &= (T^A \otimes \bar{T}^A) \left[\frac{\mathcal{V}_c^{(T)}}{\mathbf{k}^2} + \frac{\mathcal{V}_k^{(T)} \pi^2}{m|\mathbf{k}|} + \frac{\mathcal{V}_r^{(T)}(\mathbf{p}^2 + \mathbf{p}'^2)}{2m^2 \mathbf{k}^2} + \frac{\mathcal{V}_2^{(T)}}{m^2} + \frac{\mathcal{V}_s^{(T)}}{m^2} \mathbf{S}^2 \right. \\
&\quad \left. + \frac{\mathcal{V}_\Lambda^{(T)}}{m^2} \Lambda(\mathbf{p}', \mathbf{p}) + \frac{\mathcal{V}_t^{(T)}}{m^2} T(\mathbf{k}) + \dots \right] + (1 \otimes 1) \left[\frac{\mathcal{V}_c^{(1)}}{\mathbf{k}^2} + \frac{\mathcal{V}_k^{(1)} \pi^2}{m|\mathbf{k}|} + \frac{\mathcal{V}_2^{(1)}}{m^2} + \frac{\mathcal{V}_s^{(1)}}{m^2} \mathbf{S}^2 + \dots \right], \\
\mathbf{S} &= \frac{\boldsymbol{\sigma}_1 + \boldsymbol{\sigma}_2}{2}, \quad \Lambda(\mathbf{p}', \mathbf{p}) = -i \frac{\mathbf{S} \cdot (\mathbf{p}' \times \mathbf{p})}{\mathbf{k}^2}, \quad T(\mathbf{k}) = \boldsymbol{\sigma}_1 \cdot \boldsymbol{\sigma}_2 - \frac{3 \mathbf{k} \cdot \boldsymbol{\sigma}_1 \mathbf{k} \cdot \boldsymbol{\sigma}_2}{\mathbf{k}^2}, \\
F_j^{ABC}(\mathbf{p}, \mathbf{p}') &= \frac{2i \mathcal{V}_c^{(T)} \mathbf{k}_j}{\mathbf{k}^4} f^{ABC}, \tag{6}
\end{aligned}$$

where $\mathbf{k} = \mathbf{p}' - \mathbf{p}$. The factors $\mathcal{V}_j(\nu)$ are renormalized Wilson coefficients, and the coefficient $\mathcal{V}_c^{(T)}$ in F_j^{ABC} is fixed by reparameterization invariance [5] as shown in Ref. [17]. Some further operators are required to renormalize $\mathcal{L}_{s,p}$ and will be discussed later on.

It is worth noting that the factors of μ_U^ϵ and μ_S^ϵ in $\mathcal{L}_{u,s,p}$ are uniquely determined by mass dimension and v power counting in $d = 4 - 2\epsilon$ dimensions [16]. A scaling with v is assigned to the effective theory fields so that in the action their kinetic terms are order v^0 . This gives $\psi_{\mathbf{p}} \sim (mv)^{3/2-\epsilon}$, $A^\mu \sim (mv^2)^{1-\epsilon}$, and $A_q^\mu \sim (mv)^{1-\epsilon}$. Since $D^\mu \sim mv^2$, the renormalized combination $g_u A^\mu$ must be multiplied by $\mu_U^\epsilon \sim (mv)^\epsilon$ so that this gluon term also scales as mv^2 . For the potential fermion terms in \mathcal{L}_s displayed in Eq. (4) the soft and potential fields give a $(mv)^{5-4\epsilon}$ and the complete measure gives $(mv)^{-4+2\epsilon}$. The factor of $\mu_S^{2\epsilon} \sim (mv)^{2\epsilon}$ is therefore required to cancel the $v^{-2\epsilon}$ from the measure and fields. For the four-quark operator in \mathcal{L}_p the quark fields give $(mv)^{6-4\epsilon}$ and the complete measure gives $(mv^2)^{-1}(mv)^{-3+2\epsilon}$, so a factor of $\mu_S^{2\epsilon} \sim (mv)^{2\epsilon}$ multiplying $V(\mathbf{p}, \mathbf{p}')$ is required. The factors of μ_U^ϵ and μ_S^ϵ for any other operator can also be determined in this way.

The power counting of an arbitrary diagram is determined entirely by the powers of v assigned to its operators. Since the factors of μ_U^ϵ and μ_S^ϵ are already determined, we can work in $d = 4$ dimensions. In general a graph is order $\sim v^\delta$ with [14]

$$\delta = 5 + \sum_k \left[(k-8)V_k^{(u)} + (k-5)V_k^{(p)} + (k-4)V_k^{(s)} \right] - N_s. \tag{7}$$

Here N_s is the number of disconnected soft subgraphs if potential lines are erased, the vertex factors $V_k^{(i)}$ count the number of insertions of an operator scaling as v^k . The factors $V_k^{(u)}$ are for purely ultrasoft operators, $V_k^{(p)}$ are for operators which contain $\psi_{\mathbf{p}}$ or $\chi_{\mathbf{p}}$ but no soft fields, and $V_k^{(s)}$ are for operators with at least one soft field. In this paper we will refer to the order in v of diagrams and operators as their value of

$$\delta' = \delta - 5, \tag{8}$$

since this quantity is essentially additive with multiple insertions of operators [22]. For instance, using the value of δ' for the power counting a T-product of the potentials $V_1 \sim v^a$ and $V_2 \sim v^b$ scales as $T[V_1 V_2] \sim v^{a+b}$. With this counting the Coulomb potential scales as



FIG. 1: Examples of mixed soft-ultrasoft graphs with A^0 ultrasoft gluons which could renormalize \mathcal{L}_s in Feynman gauge. The zigzag lines denote soft gluons, quarks, or ghosts.

v^{-1} , the $1/|\mathbf{k}|$ potential is order v^0 and the $1/m^2$ potentials are order v^1 . For later use we also define

$$\sigma = k - 4 \quad (9)$$

as the order in v for which a soft operator contributes to the power counting formula in Eq. (7).

III. ULTRASOFT RENORMALIZATION OF OPERATORS

Since the effective theory simultaneously involves soft and ultrasoft gluons the question naturally arises in what manner the two types of gluons renormalize operators. As far as renormalization of \mathcal{L}_u is concerned the ultrasoft renormalization is equivalent to that in HQET. This is because after the equation of motion $E = \mathbf{p}^2/(2m)$ is applied, the quark propagators in loop graphs in the single fermion sector become static [14],

$$\frac{i}{E + k^0 - \mathbf{p}^2/(2m) + i\epsilon} = \frac{i}{k^0 + i\epsilon}. \quad (10)$$

Here (E, \mathbf{p}) are the energy and momentum of the external quark line. Thus, the renormalized \mathcal{L}_u is exactly of the form of the multipole-expanded renormalized HQET Lagrangian.

The ultrasoft renormalization of interactions generated by \mathcal{L}_s and \mathcal{L}_p is more subtle. The basic complication is that one must account for the fact that ultrasoft gluons renormalize operators which are non-local with respect to the mv scale (but are local relative to mv^2).

First consider the renormalization of interactions generated by \mathcal{L}_s . Directly renormalizing \mathcal{L}_s by ultrasoft gluons leads to gauge dependent Wilson coefficients as observed in Ref. [17]. To see this consider the graphs in Fig. 1 which involve ultrasoft A^0 gluons. In Coulomb gauge these graphs are identically zero. In Feynman gauge the sum of Fig. 1a and the quark wavefunction renormalization give a C_A/ϵ term which could contribute to the renormalization of $U_{\mu\nu}^{(0)}$ in \mathcal{L}_s . Non-Abelian graphs such as the one in Fig. 1b do not cancel this contribution. For Fig. 1b, the intermediate soft gluon propagator has momentum $(q + k)^2 = q^2 + 2k \cdot q + k^2$, but we cannot set the offshellness $q^2 \sim (mv)^2$ of the soft gluon to zero without violating the power counting and risking a double counting. Keeping $q^2 \neq 0$, Fig. 1b evaluates to zero and it is not surprising that the total result is gauge dependent since part of the calculation was done offshell. This issue can be avoided by only considering the ultrasoft renormalization of operators which can contribute as soft color singlets [17], such as time-ordered products involving two or more soft vertices and quarks and antiquarks, $T(\mathcal{L}_s^\psi \mathcal{L}_s^\chi \dots)$. These products appear local as far as the ultrasoft gluon is concerned, and it is only these products which affect observables. Having ultrasoft renormalization only for these operators also avoids the predicament of having both ultrasoft and soft gluons in the

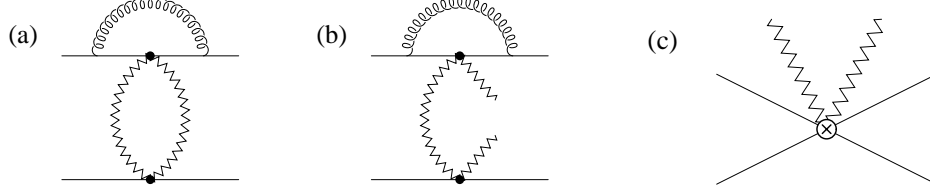


FIG. 2: The zigzag lines denote soft gluons, quarks, or ghosts. Graphs (a) and (b) are examples of mixed soft-soft graphs, while (c) denotes an operator for soft Compton scattering off a potential.

single heavy quark sector. Thus, we do not consider ultrasoft renormalization of a single \mathcal{L}_s term.

However this does *not* imply that the first ultrasoft renormalization of a graph involving soft vertices are for two loops graphs like the one in Fig. 2a. The reason is that we must first consider the case where only one pair of soft gluon fields in the time-ordered product are contracted. So at one-loop we must consider the renormalization of graphs such as the one shown in Fig. 2b. The ultraviolet divergences in these graphs need to be canceled by counterterms for the 6-field operators, $\mathcal{O}_{2i}^{(\sigma)}$ shown in Fig. 2c. For quarks, gluons, and ghosts these operators have the structure

$$\begin{aligned}\mathcal{O}_{2\varphi}^{(\sigma)} &= g_s^4 \mu_S^{4\epsilon} (\psi_{\mathbf{p}'}^\dagger \Gamma_{\varphi,\psi}^{(\sigma)} \psi_{\mathbf{p}}) (\chi_{-\mathbf{p}'}^\dagger \Gamma_{\varphi,\chi}^{(\sigma)} \chi_{-\mathbf{p}}) (\bar{\varphi}_{-q} \Gamma_{\varphi}^{(\sigma)} \varphi_q), \\ \mathcal{O}_{2A}^{(\sigma)} &= g_s^4 \mu_S^{4\epsilon} (\psi_{\mathbf{p}'}^\dagger \Gamma_{A,\psi}^{(\sigma)} \psi_{\mathbf{p}}) (\chi_{-\mathbf{p}'}^\dagger \Gamma_{A,\chi}^{(\sigma)} \chi_{-\mathbf{p}}) (A_{-q}^\mu \Gamma_{A,\mu\nu}^{(\sigma)} A_q^\nu), \\ \mathcal{O}_{2c}^{(\sigma)} &= g_s^4 \mu_S^{4\epsilon} (\psi_{\mathbf{p}'}^\dagger \Gamma_{c,\psi}^{(\sigma)} \psi_{\mathbf{p}}) (\chi_{-\mathbf{p}'}^\dagger \Gamma_{c,\chi}^{(\sigma)} \chi_{-\mathbf{p}}) (\bar{c}_{-q} \Gamma_c^{(\sigma)} c_q),\end{aligned}\tag{11}$$

where color indices are suppressed and the factor of $\mu_S^{4\epsilon}$ is determined by the procedure in Sect. II. Here the Γ_i are matrices in spin and/or color space and can be functions of \mathbf{p}' , \mathbf{p} , and q^μ . This soft momentum dependence is identical to that in the graph on the LHS of Fig. 3 once the equations of motion are applied (e.g. $q^2 = 0$, $\not{q}\varphi_q = 0$). The superscript $\sigma \geq 0$ has been used in Eq. (9) and denotes the order in v for which these soft operators contribute to the power counting in Eq. (7). For our purposes the $\sigma = 0, 2$ operators will be sufficient. The operators in Eq. (11) also have Wilson coefficients $C_{2i}^{(\sigma)}(\nu)$. The tricky thing about the operators $\mathcal{O}_{2i}^{(\sigma)}$ is that the tree level matching onto their Wilson coefficients is zero, $C_{2i}^{(\sigma)}(\nu = 1) = 0$. An example of this matching calculation is shown in Fig. 3 for $\mathcal{O}_{2\varphi}^{(\sigma)}$. At $\nu = 1$ the full theory graph on the left is exactly canceled by the time ordered product of soft vertices. Therefore, we get zero for the Wilson coefficient of the operator on the right. However, the ultrasoft loop graph in Fig. 2b gives $\mathcal{O}_{2i}^{(2)}$ a non-zero anomalous dimension so that for $\nu < 1$ the coefficient evolves and $C_{2i}^{(2)}(\nu < 1) \neq 0$. The same counterterm is necessary to renormalize the divergences in Fig 2a. Furthermore, the operators $\mathcal{O}_{2i}^{(2)}$ affect the anomalous dimensions for the $1/m^2$ coefficients \mathcal{V}_2 and \mathcal{V}_r in Eq. (6), and were not included in Ref. [15]. This occurs through an ultraviolet divergence in the graph in Fig. 5c which needs to be canceled by $\mathcal{V}_{2,r}$ counterterms. In Secs. IV and V we will give two examples of the implications of the operators in Eq. (11).

Let us now discuss the ultrasoft renormalization for two-body interactions generated by \mathcal{L}_p . In general in graphs with two heavy quarks the equations of motion do not make the propagators static. For example, in the order v^0 two-loop graph in Fig. 4a the ultrasoft loop

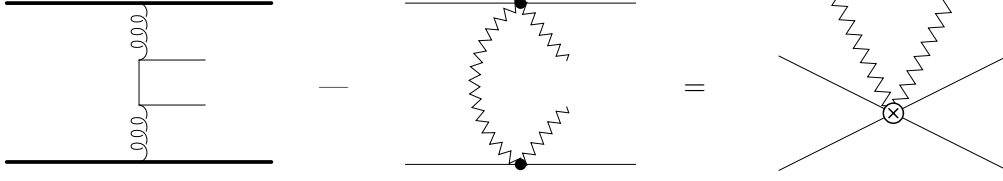


FIG. 3: Example of the matching calculation for $\mathcal{O}_{2\varphi}^{(\sigma)}$. Here the zig-zag lines denote soft massless fermions. At the high scale ($\nu = 1$) the graphs on the left exactly cancel so the coefficient of the operator on the right is zero.

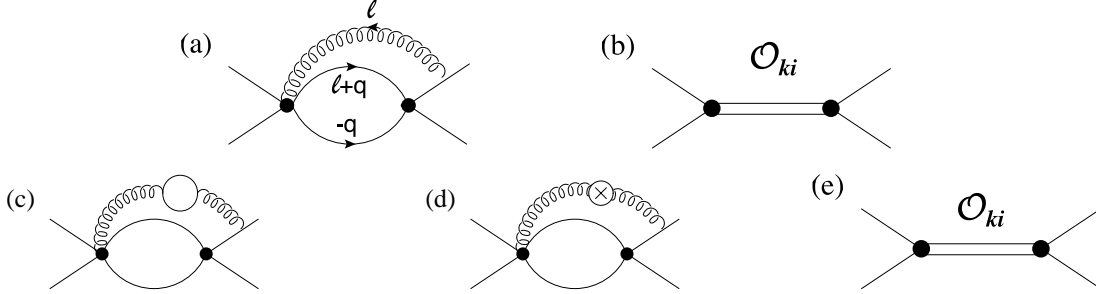


FIG. 4: Example of renormalization of two-body potential graphs by an ultrasoft gluon. The ultrasoft couplings are the order v^0 term from Eq. (5) and the order v^1 term $\mathbf{p} \cdot \mathbf{A}$ in Eq. (3).

momentum ℓ^μ is routed through an internal fermion line giving a propagator

$$\frac{i}{E + \ell^0 + q^0 - \mathbf{q}^2/(2m) + i\epsilon} = \frac{i}{\ell^0 + q^0 - (\mathbf{q}^2 - \mathbf{p}^2)/(2m) + i\epsilon}, \quad (12)$$

where $q = (q^0, \mathbf{q})$ is the potential loop momentum. The multipole expansion has resulted in factors of the three-momentum ℓ being dropped, however the remaining propagator is not static in general since $\mathbf{q}^2 \neq \mathbf{p}^2$. In fact, the ultrasoft loop induces an UV divergence after the dq^0 and $d\ell$ integrals have been performed, but before the sum over indices \mathbf{q} is carried out. In Refs. [17, 18] the subtraction of the ultrasoft UV divergences was made after carrying out the sum over \mathbf{q} . Instead, the corresponding operators used to subtract the divergences should involve a sum over \mathbf{q} . For example, for the sum of all scattering diagrams at order $\alpha_s^3 v^0$ with one ultrasoft gluon the operators needed to subtract the ultrasoft UV divergences have the form

$$\begin{aligned} \mathcal{O}_{k1}^{(1)} &= -\frac{[\mu_S^{2\epsilon} \mathcal{V}_c^{(T)}]^2}{m} \sum_{\mathbf{p}, \mathbf{p}', \mathbf{q}} (f_0 + f_1 + 2f_2) [\psi_{\mathbf{p}}^\dagger \psi_{\mathbf{p}} \chi_{-\mathbf{p}'}^\dagger \chi_{-\mathbf{p}}], \\ \mathcal{O}_{k2}^{(T)} &= -\frac{[\mu_S^{2\epsilon} \mathcal{V}_c^{(T)}]^2}{m} \sum_{\mathbf{p}, \mathbf{p}', \mathbf{q}} (f_1 + f_2) [\psi_{\mathbf{p}}^\dagger T^A \psi_{\mathbf{p}} \chi_{-\mathbf{p}'}^\dagger \bar{T}^A \chi_{-\mathbf{p}}], \end{aligned} \quad (13)$$

where the f_i are functions of \mathbf{p}, \mathbf{p}' and \mathbf{q} that will be given in Sec. VI. These operators are denoted graphically by the diagram in Fig. 4b, since they are essentially like the product of two potentials summed over the intermediate 3-momentum \mathbf{q} . A similar set of operators exists for three-loop diagrams with an ultrasoft gluon at order $\alpha_s^4 v^{-1}$. To evaluate matrix elements of these operators using dimensional regularization we combine the sums with the

integration over the ultrasoft spacetime coordinate x [14], which leads to

$$\sum_{\mathbf{q}} \rightarrow \int d^{d-1}q. \quad (14)$$

Unlike the sums over labels on the fields, the free sum over \mathbf{q} scales as $v^{-2\epsilon}$, and contributes in determining the factor of $\mu_S^{4\epsilon}$ in Eq. (13).

At the level of Fig. 4a it still appears ambiguous whether the sum over \mathbf{q} in Eq. (13) needs to be carried out. The key point is that the original ultrasoft divergent loop in Fig. 4a acts like a one-loop subdivergence, despite the fact that it shows up at the level of the two loop graph. Therefore, it renormalizes each term in the sum of the operators in Eq. (13), rather than a potential $V(\mathbf{p}, \mathbf{p}')$ with the sum over \mathbf{q} already carried out.

This renormalization prescription can be illustrated by considering a graph with an additional ultrasoft fermion bubble as in Fig. 4c. To renormalize Fig. 4c we require both the $1/\epsilon$ counterterm for the fermion bubble as in Fig. 4d, and a $1/\epsilon^2$ counterterm from Fig. 4e. which has an identical momentum structure to the operators in Fig. 4b. In dimensional regularization the complete result for the sum of the three graphs has the divergent structure

$$\left(\frac{\mu_S^2}{\mathbf{k}^2}\right)^\epsilon \left[\frac{1}{2\epsilon^2} \left(\frac{\mu_U^2}{E^2}\right)^{2\epsilon} - \frac{1}{\epsilon^2} \left(\frac{\mu_U^2}{E^2}\right)^\epsilon + \frac{1}{2\epsilon^2} \right], \quad (15)$$

where in the limit $\epsilon \rightarrow 0$ all possible subdivergences $\ln(E^2/\mu_U^2)/\epsilon$ and $\ln(\mathbf{k}^2/\mu_S^2)/\epsilon$ are canceled by the counterterm contributions. If we only needed counterterms to be added after the sum on \mathbf{q} was carried out then the sum of Figs. 4c and 4d

$$\left(\frac{\mu_S^2}{\mathbf{k}^2}\right)^\epsilon \left[\frac{1}{2\epsilon^2} \left(\frac{\mu_U^2}{E^2}\right)^{2\epsilon} - \frac{1}{\epsilon^2} \left(\frac{\mu_U^2}{E^2}\right)^\epsilon \right] = -\frac{1}{2\epsilon^2} - \frac{1}{2\epsilon} \ln\left(\frac{\mu_S^2}{\mathbf{k}^2}\right) + \dots, \quad (16)$$

should only contain an overall analytic divergence. However, Eq. (16) has a non-analytic divergence. We note that as for the operators $\mathcal{O}_{2i}^{(\sigma)}$ the Wilson coefficients $\mathcal{V}_{ki}(\nu)$ of the operators \mathcal{O}_{ki} vanish at the hard scale, i.e. $\mathcal{V}_{ki}(\nu = 1) = 0$. However, divergences from graphs such as those in Fig. 4 lead to a non-zero anomalous dimension so that $\mathcal{V}_{ki}(\nu < 1) \neq 0$. Furthermore we emphasize that the renormalization of these operators is not equivalent to the renormalization of the QCD $1/|\mathbf{k}|$ and $1/\mathbf{k}^2$ potentials or to the renormalization of $1/r$ or $1/r^2$ potentials. This will be discussed further in Sec. VI.

IV. MUONIC-HYDROGEN WITH MASSLESS ELECTRONS

Our first example is a simplified toy model for muonic-Hydrogen with proton mass $m_p \rightarrow \infty$, muon mass m fixed, and n_f massless “electrons”. In this theory the running of the coupling is simplified because there are no gauge boson self interactions. Furthermore at the order we are working the soft graphs simply involve massless leptons. This model was proposed in Refs. [24, 27] as a test of the anomalous dimensions of the $1/m^2$ operators (see also Ref. [26] and reference one in [1]). In this section we show that vNRQCD correctly reproduces the $n_f \alpha^6 \ln^2 \alpha$ energy levels in this toy model and is therefore in agreement with the QED limit of Pachuki’s results in Ref. [28].

For this toy model we have $(T^A \otimes \bar{T}^A) \rightarrow (-1)$, $(1 \otimes 1) \rightarrow (+1)$ and therefore define $\mathcal{V}_i = \mathcal{V}_i^{(1)} - \mathcal{V}_i^{(T)}$. For the soft spin-independent vertices with $m_p = \infty$ we only require

$Z_0^{(0)} = 1/\mathbf{k}^2$ and $Z_0^{(2)} = -c_D(m\nu)/(8m^2)$ from Ref. [15]. Here $c_D(\mu)$ is the QED limit of the gauge invariant Darwin coefficient computed in Ref. [29],

$$c_D(\mu) = 1 + \frac{16}{3\bar{\beta}_0} \ln \left[\frac{\alpha(\mu)}{\alpha(m)} \right], \quad (17)$$

where $\bar{\beta}_0 = -4n_f/3$. The operator $\mathcal{O}_{2\varphi}^{(0)}$ has the form

$$\mathcal{O}_{2\varphi}^{(0)} = e^4 \mu_S^{4\epsilon} (\psi_{\mathbf{p}'}^\dagger \Gamma_\psi^{(0)} \psi_{\mathbf{p}}) (\chi_{-\mathbf{p}'}^\dagger \Gamma_\chi^{(0)} \chi_{-\mathbf{p}}) (\bar{\varphi}_{-q} \Gamma_\varphi^{(0)} \varphi_q), \quad (18)$$

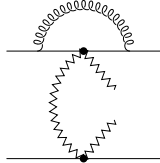
where

$$\begin{aligned} \Gamma_\varphi^{(0)}(q, \mathbf{p}, \mathbf{p}') &= \left[\frac{(2q^0 \gamma^0 + \mathbf{k} \cdot \boldsymbol{\gamma})}{\mathbf{k}^2 + 2\mathbf{k} \cdot \mathbf{q}} + \frac{(2q^0 \gamma^0 - \mathbf{k} \cdot \boldsymbol{\gamma})}{\mathbf{k}^2 - 2\mathbf{k} \cdot \mathbf{q}} \right] \left(Z_0^{(0)} \right)^2, \\ \Gamma_{\varphi, \psi}^{(0)} &= 1, \quad \Gamma_{\varphi, \chi}^{(0)} = -1, \end{aligned} \quad (19)$$

and $\mathbf{k} = \mathbf{p}' - \mathbf{p}$. From tree level matching we have $C_{2\varphi}^{(0)}(1) = 0$. Furthermore, since ultrasoft photons bring an extra v^2 , there is no anomalous dimension induced for this coefficient, so in fact $C_{2\varphi}^{(0)}(\nu) = 0$ and this operator does not need to be considered further. The operator $\mathcal{O}_{2\varphi}^{(2)}$ has the form

$$\mathcal{O}_{2\varphi}^{(2)} = -\frac{\mathbf{k}^2}{6m^2} \mathcal{O}_{2\varphi}^{(0)}. \quad (20)$$

From tree level matching one finds that its coefficient vanishes also at the hard scale, $C_{2\varphi}^{(2)}(1) = 0$, but it gets a non-trivial anomalous dimension from the UV divergences in the ultrasoft graph in Fig. 2b plus wavefunction counterterms,



$$+ \text{w.fn.} = -\frac{1}{6\pi} \frac{\mathbf{k}^2}{m^2} \frac{\alpha(m\nu^2)}{\epsilon} \langle i\mathcal{O}_{2\varphi}^{(0)} \rangle_{4e2\gamma} = \frac{1}{\pi} \frac{\alpha(m\nu^2)}{\epsilon} \langle i\mathcal{O}_{2\varphi}^{(2)} \rangle_{4e2\gamma}, \quad (21)$$

where the soft vertices symbolized by the dots stand for the coupling $Z_0^{(0)}$. Together with the respective soft divergence induced by the pull-up mechanism [18] this gives

$$\frac{1}{\pi} \left[\frac{\alpha(m\nu^2)}{\epsilon} - \frac{\alpha(m\nu)}{\epsilon} \right] \langle i\mathcal{O}_{2\varphi}^{(2)} \rangle_{4e2\gamma}. \quad (22)$$

We see that the result would vanish if the two couplings were evaluated at the same scale. The result in Eq. (22) is canceled by a counterterm for $C_{2\varphi}^{(2)}$ which, using the vRGE, gives the anomalous dimension

$$\nu \frac{\partial}{\partial \nu} C_{2\varphi}^{(2)} = -\frac{2}{\pi} \left[2\alpha(m\nu^2) - \alpha(m\nu) \right]. \quad (23)$$

There is another possible contribution to the anomalous dimension in Eq. (23) coming from the soft coupling renormalization graphs for the operator $\mathcal{O}_{2\varphi}^{(2)}$, however these are exactly

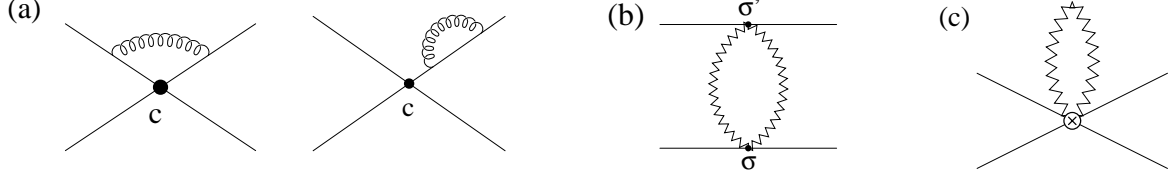


FIG. 5: a) ultrasoft gluon graphs with $\mathbf{p} \cdot \mathbf{A}$ vertices (with wavefunction renormalization on the other line understood), b) soft graph with $Z_0^{(\sigma=0)}$ and $Z_0^{(\sigma'=2)}$ vertices, c) soft graph involving $\mathcal{O}_{2\varphi}^{(2)}$. The zig-zag lines here denote massless soft fermions.

canceled by the charge counterterm contribution associated to the factor e^4 in Eq.(18). Similarly, an UV divergence in the analogue of Fig. 2b having only soft gluons is exactly canceled by a counterterm associated to the $Z_0^{(2)}$ term in the soft Lagrangian. Solving Eq. (23) with the boundary condition $C_{2\varphi}^{(2)}(1) = 0$ gives

$$C_{2\varphi}^{(2)}(\nu) = \frac{4}{\beta_0} \ln \left[\frac{\alpha(m\nu^2)}{\alpha(m\nu)} \right] = \frac{3}{4} \left[c_D(m\nu^2) - c_D(m\nu) \right]. \quad (24)$$

The anomalous dimension for \mathcal{V}_2 can now be computed from the graphs in Fig. 5 which are order $v^1 e^4$. The graphs in Fig. 5a, 5b, 5c give the following three terms

$$\nu \frac{\partial}{\partial \nu} \mathcal{V}_2 = -\frac{8}{3} \alpha(m\nu) \alpha(m\nu^2) + \frac{n_f}{3} c_D(m\nu) [\alpha(m\nu)]^2 + \frac{4n_f}{9} C_{2\varphi}^{(2)}(\nu) [\alpha(m\nu)]^2. \quad (25)$$

Using the solution in Eq. (24) this becomes

$$\nu \frac{\partial}{\partial \nu} \mathcal{V}_2 = -\frac{8}{3} \alpha(m\nu) \alpha(m\nu^2) + \frac{n_f}{3} c_D(m\nu^2) [\alpha(m\nu)]^2. \quad (26)$$

Solving this equation with the boundary condition $\mathcal{V}_2(1) = \pi\alpha(m)/2$ we find

$$\mathcal{V}_2(\nu) = \frac{\pi}{2} c_D(m\nu^2) \alpha(m\nu). \quad (27)$$

The result differs from the coefficient of the four quark operator in Ref. [26] in mNRQCD ($m\nu < \mu < m$). Our result is in agreement with the pNRQCD result in Ref. [26]

$$\pi D_d^{(2)}(\nu_{us}) = \frac{\pi}{2} c_D(\nu_{us}) \alpha(r^{-1}), \quad (28)$$

but only if we correlate the mNRQCD–pNRQCD matching scale $1/r$ with the pNRQCD renormalization scale ν_{us} for the energy by enforcing $\nu_{us} = m\nu^2$ and $1/r = m\nu$. We also agree with Pachucki [28] for the $n_f \alpha^6 \ln^2 \alpha$ energy levels for this toy model. In Ref. [26] a different expression for $\mathcal{V}_2(\nu)$ was inferred for the vNRQCD approach, however this is because the contribution from the graph in Fig. 5c was missing.

V. QCD RESULTS FOR $1/m^2$ POTENTIALS

Our second example of the effect of the operators in Eq. (11) is non-relativistic QCD for equal mass heavy fermions. In this case the soft degrees of freedom include soft gluons,

quarks, and ghosts. The operators $\mathcal{O}_{2\varphi}^{(0)}$, $\mathcal{O}_{2A}^{(0)}$ and $\mathcal{O}_{2c}^{(0)}$ can be written in a compact form in terms of the soft vertices $U_{\mu\nu}^{(0)}$, $Y^{(0)}$, and $Z^{(0)}$ from Ref. [15], as summarized in Appendix A. Closing the respective two soft (gluon, quark and ghost) lines one obtains for the one-loop four quark matrix element a structure that is identical to the one-loop time-ordered product of the soft vertices $U_{\mu\nu}^{(0)}$, $Y^{(0)}$, and $Z^{(0)}$ [up to non-trivial Wilson coefficients which are suppressed in this equality]:

$$\begin{aligned}
\text{Diagram} &= \langle i\mathcal{O}_{2A}^{(0)} \rangle_{4Q} + \langle i\mathcal{O}_{2c}^{(0)} \rangle_{4Q} + \langle i\mathcal{O}_{2\varphi}^{(0)} \rangle_{4Q} = \sum_i \langle i\mathcal{O}_{2i}^{(0)} \rangle_{4Q} \\
&= -i \frac{\beta_0 \alpha_s (m\nu)^2}{\mathbf{k}^2 \epsilon} T^A \otimes \bar{T}^A + \dots = \text{Diagram} . \tag{29}
\end{aligned}$$

Just as in the matching calculation for the QED toy model the momentum structure of the soft time-ordered products agrees with the full theory result, so at $\nu = 1$ we find $C_{2i}^{(0)}(1) = 0$. Similarly, since ultrasoft gluons bring an extra factor v^2 there is again no anomalous dimension induced for the operators $\mathcal{O}_{2i}^{(0)}$ and we have $C_{2i}^{(0)}(\nu) = 0$ identically.

For $\sigma = 2$ it is necessary to keep the different color structures between the heavy fermions, so in general we have to consider two types of operators, $\mathcal{O}_{2i}^{(2),(T)}$ with the fermionic structure $[\psi_{\mathbf{p}}^\dagger T^A \psi_{\mathbf{p}} \chi_{-\mathbf{p}}^\dagger \bar{T}^A \chi_{-\mathbf{p}}]$ and $\mathcal{O}_{2i}^{(2),(1)}$ with the fermionic structure $[\psi_{\mathbf{p}}^\dagger \psi_{\mathbf{p}} \chi_{-\mathbf{p}}^\dagger \chi_{-\mathbf{p}}]$. These operators are defined by Eq. (32) with $\mathcal{O}_{2i}^{(0),(1,T)}$ defined in Appendix A. For our purposes it is sufficient to consider only operators where the soft lines are closed in color space, and the operators $\mathcal{O}_{2i}^{(0),(1,T)}$ and $\mathcal{O}_{2i}^{(2),(1,T)}$ are defined with this convention. This is sufficient because for the renormalization of the potentials all external soft lines are contracted. From tree level matching one obtains that the coefficients of these operators vanish at the hard scale $C_{2i}^{(2),(T)}(1) = C_{2i}^{(2),(1)}(1) = 0$, but as in the QED case they have a non-vanishing anomalous dimension due to the exchange of ultrasoft gluons in diagrams of order $\alpha_s^2 v^1$ as shown in Fig. 2b. Now since we are dealing with equal mass fermions, the $\mathbf{p} \cdot \mathbf{A}$ ultrasoft gluons can attach to any of the heavy fermion lines. Including the permutations of possible ultrasoft attachments we find

$$\begin{aligned}
\text{Diagram 1} + \text{Diagram 2} + \dots &= \frac{\alpha_s (m\nu^2)}{\pi \epsilon} \sum_i \left\{ \frac{C_1}{3} \frac{\mathbf{k}^2}{m^2} \langle i\mathcal{O}_{2i}^{(0),(1)} \rangle_{4Q2i} - \left[C_A \frac{(\mathbf{p}^2 + \mathbf{p}'^2)}{3m^2} \right. \right. \\
&\quad \left. \left. + \left(\frac{C_F}{3} + \frac{C_d}{12} - \frac{C_A}{4} \right) \frac{\mathbf{k}^2}{m^2} \right] \langle i\mathcal{O}_{2i}^{(0),(T)} \rangle_{4Q2i} \right\}, \tag{30}
\end{aligned}$$

where the ellipses denote other attachments including wavefunction diagrams. For $\text{SU}(N_c)$ QCD the color coefficients that appear here are

$$C_A = N_c, \quad C_F = \frac{N_c^2 - 1}{2N_c}, \quad C_d = 8C_F - 3C_A, \quad C_1 = \frac{1}{2} C_F C_A - C_F^2. \tag{31}$$

The result in Eq. (30) renormalizes the operators

$$\begin{aligned}\mathcal{O}_{2a}^{(2),(1)} &= \frac{\mathbf{k}^2}{m^2} \sum_i \mathcal{O}_{2i}^{(0),(1)}, \quad \mathcal{O}_{2b}^{(2),(T)} = \frac{\mathbf{k}^2}{m^2} \sum_i \mathcal{O}_{2i}^{(0),(T)}, \\ \mathcal{O}_{2c}^{(2),(T)} &= \frac{(\mathbf{p}^2 + \mathbf{p}'^2)}{m^2} \sum_i \mathcal{O}_{2i}^{(0),(T)},\end{aligned}\tag{32}$$

whose coefficients $C_{2a}^{(2)}$, $C_{2b}^{(2)}$, and $C_{2c}^{(2)}$ vanish at the matching scale $\nu = 1$. Adding to Eq. (30) the soft divergences induced by the pull-up mechanism one arrives at the following anomalous dimension for the coefficients:

$$\begin{aligned}\nu \frac{\partial}{\partial \nu} C_{2a}^{(2)} &= \frac{-2C_1}{3\pi} \gamma_{u2}(\nu), \quad \nu \frac{\partial}{\partial \nu} C_{2b}^{(2)} = \frac{4C_F + C_d - 3C_A}{6\pi} \gamma_{u2}(\nu), \quad \nu \frac{\partial}{\partial \nu} C_{2c}^{(2)} = \frac{2C_A}{3\pi} \gamma_{u2}(\nu), \\ \gamma_{u2}(\nu) &\equiv 2\alpha_s(m\nu^2) - \alpha_s(m\nu).\end{aligned}\tag{33}$$

These equations are quite similar to Eq. (23) and their solutions are

$$\begin{aligned}C_{2a}^{(2)}(\nu) &= \frac{4C_1}{3\beta_0} \ln(w), \quad C_{2b}^{(2)}(\nu) = \frac{3C_A - C_d - 4C_F}{3\beta_0} \ln(w), \\ C_{2c}^{(2)}(\nu) &= \frac{-4C_A}{3\beta_0} \ln(w),\end{aligned}\tag{34}$$

where

$$w = \frac{\alpha_s(m\nu^2)}{\alpha_s(m\nu)}.\tag{35}$$

Note that as in the QED case there are additional possible contributions to the anomalous dimensions of the operators $\mathcal{O}_{2i}^{(2),(1,T)}$ which are, however, exactly canceled by pre-existing counterterms. This includes for example the purely soft diagram analogous to Fig. 2b, and the soft coupling renormalization graphs. The divergences of the soft diagrams are canceled by counterterms for $U_{\mu\nu}^{(2)}$, $Z_0^{(2)}$, $Y^{(2)}$ and the divergences of the soft coupling graphs by the counterterm associated to the factor g_s^4 in Eq. (11).

Finally, we consider the anomalous dimensions for the spin-independent potential coefficients $\mathcal{V}_{2,r}^{(1,T)}(\nu)$. The graphs required for this computation are shown in Fig. 6. The graphs in Fig. 6a and 6b were computed in Ref. [15], however the contributions from the graph in Fig. 6c which are proportional to the coefficients $C_{2i}^{(2)}$ were not included. Adding the contributions from all three graphs the results are

$$\begin{aligned}\nu \frac{\partial}{\partial \nu} \mathcal{V}_r^{(T)} &= -2(\beta_0 + \frac{8}{3}C_A) \alpha_s^2(m\nu) + \frac{32}{3}C_A \alpha_s(m\nu) \alpha_s(m\nu^2) - 4\beta_0 C_{2c}^{(2)}(\nu) \alpha_s(m\nu)^2, \\ \nu \frac{\partial}{\partial \nu} \mathcal{V}_2^{(T)} &= \left\{ \frac{\beta_0}{2} [1 + c_D(\nu) - 2c_F^2(\nu)] + \frac{C_A}{6} [28 - 11c_D(\nu) + 26c_F(\nu)^2] - \frac{7C_d}{6} \right\} \alpha_s^2(m\nu) \\ &\quad + \frac{4}{3}(4C_F + C_d - 3C_A) \alpha_s(m\nu) \alpha_s(m\nu^2) - 2\beta_0 C_{2b}^{(2)}(\nu) \alpha_s(m\nu)^2, \\ \nu \frac{\partial}{\partial \nu} \mathcal{V}_2^{(1)} &= \frac{14}{3} C_1 \alpha_s^2(m\nu) - \frac{16}{3} C_1 \alpha_s(m\nu) \alpha_s(m\nu^2) - 2\beta_0 C_{2a}^{(2)}(\nu) \alpha_s(m\nu)^2.\end{aligned}\tag{36}$$

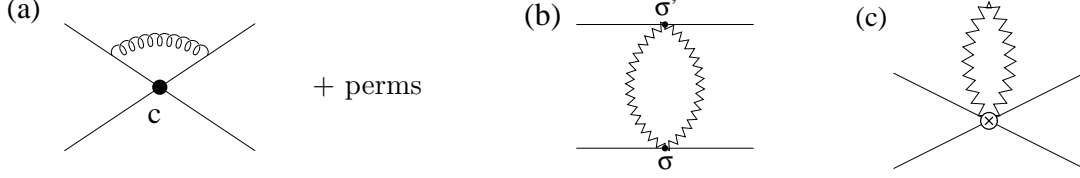


FIG. 6: a) ultrasoft gluon graphs with $\mathbf{p} \cdot \mathbf{A}$ vertices on all permutations of the four fermion lines, b) soft graph with $Z_0^{(\sigma, \sigma')}$, $U_{\mu\nu}^{(\sigma, \sigma')}$ or $Y^{(\sigma, \sigma')}$ vertices such that $\sigma + \sigma' = 2$, c) soft graph involving one of the $\mathcal{O}_{2a}^{(2)}$, $\mathcal{O}_{2b}^{(2)}$, $\mathcal{O}_{2c}^{(2)}$ operators.

The gauge invariant HQET coefficients that appear here are [29]

$$c_F(\nu) = z^{-C_A/\beta_0}, \quad c_D(\nu) = z^{-2C_A/\beta_0} + \left(\frac{20}{13} + \frac{32C_F}{13C_A} \right) [1 - z^{-13C_A/(6\beta_0)}], \quad (37)$$

where $z = \alpha_s(m\nu)/\alpha_s(m)$. The solutions for the coefficients in Eq. (36) are

$$\begin{aligned} \mathcal{V}_r^{(T)}(\nu) &= 4\pi \alpha_s(m) z - \frac{32\pi C_A}{3\beta_0} \alpha_s(m) z \ln(w), \\ \mathcal{V}_2^{(T)}(\nu) &= \frac{\pi [C_A(48C_F + 13C_d + 4C_A) - \beta_0(33C_A + 32C_F)]}{13\beta_0 C_A} \alpha_s(m) (z - 1) \\ &\quad + \frac{8\pi(3\beta_0 - 11C_A)(5C_A + 8C_F)}{13C_A(6\beta_0 - 13C_A)} \alpha_s(m) [z^{1-13C_A/(6\beta_0)} - 1] \\ &\quad + \frac{\pi(\beta_0 - 5C_A)}{(\beta_0 - 2C_A)} \alpha_s(m) [z^{1-2C_A/\beta_0} - 1] - \frac{4\pi(4C_F + C_d - 3C_A)}{3\beta_0} \alpha_s(m) z \ln(w), \\ \mathcal{V}_2^{(1)}(\nu) &= \frac{4\pi C_1}{\beta_0} \alpha_s(m) (1 - z) + \frac{16\pi C_1}{3\beta_0} \alpha_s(m) z \ln(w). \end{aligned} \quad (38)$$

For the color singlet channel $\mathcal{V}_i^{(s)} = \mathcal{V}_i^{(1)} - C_F \mathcal{V}_i^{(T)}$ and the above results give

$$\begin{aligned} \mathcal{V}_r^{(s)}(\nu) &= -4\pi C_F \alpha_s(m) z \left[1 - \frac{8C_A}{3\beta_0} \ln(w) \right], \\ \mathcal{V}_2^{(s)}(\nu) &= \pi C_F \alpha_s(m) (z - 1) \left[\frac{33}{13} + \frac{32C_F}{13C_A} + \frac{9C_A}{13\beta_0} - \frac{100C_F}{13\beta_0} \right] \\ &\quad - \frac{8\pi C_F(3\beta_0 - 11C_A)(5C_A + 8C_F)}{13C_A(6\beta_0 - 13C_A)} \alpha_s(m) [z^{1-(13C_A)/(6\beta_0)} - 1] \\ &\quad - \frac{\pi C_F(\beta_0 - 5C_A)}{(\beta_0 - 2C_A)} \alpha_s(m) [z^{1-2C_A/\beta_0} - 1] - \frac{16\pi C_F(C_A - 2C_F)}{3\beta_0} \alpha_s(m) z \ln(w). \end{aligned} \quad (39)$$

The results in Eqs. (38) and (39) are valid for all values of ν between 1 and a v_0 of order the physical velocity of the quarks. This accounts for energy scales between m and mv^2 and momentum scales between m and mv , so our results apply to this *entire* region. Our results do not agree with the running of the 4-quark operators d_{ss} , d_{sv} , d_{vs} , d_{vv} obtained in Ref. [24] for $mv < \mu < m$ (mNRQCD). This is because in Ref. [24] ultrasoft gluons are not included in the results for $\mu > mv$. To translate the results in Ref. [24] for scales $\mu < mv$ we

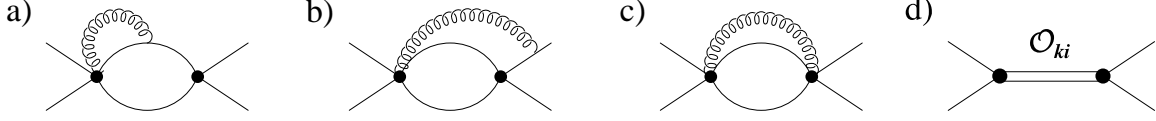


FIG. 7: Ultrasoft graphs for the renormalization of the operators $\mathcal{O}_{k1}^{(1,T)}$ (left-right and up-down symmetric graphs are implied).

note that $\mathcal{V}_r^{(s)} = -4\pi C_F D_{1,s}^{(2)}$, $\mathcal{V}_2^{(s)} = \pi C_F (D_{d,s}^{(2)} - D_{2,s}^{(2)})$, and we again enforced a correlation by demanding that the pNRQCD renormalization scale $\nu_{us} = m\nu^2$, and the mNRQCD–pNRQCD matching scale $1/r = m\nu$. With these restrictions our results in Eq. (39) agree with Ref. [24] for the case $\mu < m\nu$.

Note that there are also constraints on the relation between the cutoff for the momentum \mathbf{p} of the quarks and the cutoff for the momentum transfers $\mathbf{k} = \mathbf{p}' - \mathbf{p}$. Reproducing the known $\alpha^7 \ln^2 \alpha$ hyperfine splitting for positronium [30], requires that the cutoffs for these scales are correlated, since the calculation depends on simultaneously integrating anomalous dimensions that arise from soft and potential loops [22].

The remaining coefficients of the $1/m^2$ potentials are spin-dependent and not affected by the operator in Fig. 2c. They were computed in Ref. [15]:

$$\begin{aligned}\mathcal{V}_s^{(T)}(\nu) &= \frac{2\pi}{(2C_A - \beta_0)} \alpha_s(m) \left[C_A + \frac{1}{3}(2\beta_0 - 7C_A) z^{(1-2C_A/\beta_0)} \right], \\ \mathcal{V}_t^{(T)}(\nu) &= -\frac{\pi}{3} \alpha_s(m) z^{(1-2C_A/\beta_0)}, \\ \mathcal{V}_\Lambda^{(T)}(\nu) &= 2\pi \alpha_s(m) [z - 4 z^{(1-C_A/\beta_0)}].\end{aligned}\tag{40}$$

These expressions for $\mathcal{V}_t^{(T)}$ and $\mathcal{V}_\Lambda^{(T)}$ agree with Ref. [31] (however $\mathcal{V}_s^{(T)}$ disagrees). The results for the coefficients in Eq. (40) were confirmed in Ref. [24].

VI. QCD RESULTS FOR OPERATORS \mathcal{O}_{ki} , \mathcal{O}_{ci} AND $1/|\mathbf{k}|$, $1/\mathbf{k}^2$ POTENTIALS

At order $\alpha^3 v^0$ there are three diagrams which have ultrasoft gluons (shown in Figs. 7a,b,c) whose divergences are not canceled by counterterms from $\mathcal{V}_{2,r}$ [17]. As pointed out in Sec. III these diagrams should be renormalized by operators that do not have the sum over intermediate potential quark 3-momenta \mathbf{q} carried out, as pictured in Fig. 7d. Evaluating Figs. 7a,b,c we find that the required operators have the form

$$\begin{aligned}\mathcal{O}_{k1}^{(1)} &= -\frac{[\mu_S^{2\epsilon} \mathcal{V}_c^{(T)}]^2}{m} \sum_{\mathbf{p}, \mathbf{p}', \mathbf{q}} (f_0 + f_1 + 2f_2) [\psi_{\mathbf{p}'}^\dagger \psi_{\mathbf{p}} \chi_{-\mathbf{p}'}^\dagger \chi_{-\mathbf{p}}], \\ \mathcal{O}_{k2}^{(T)} &= -\frac{[\mu_S^{2\epsilon} \mathcal{V}_c^{(T)}]^2}{m} \sum_{\mathbf{p}, \mathbf{p}', \mathbf{q}} (f_1 + f_2) [\psi_{\mathbf{p}'}^\dagger T^A \psi_{\mathbf{p}} \chi_{-\mathbf{p}'}^\dagger \bar{T}^A \chi_{-\mathbf{p}}],\end{aligned}\tag{41}$$

giving the contribution $\Delta\mathcal{L}_p = \mathcal{V}_{k1}^{(1)} \mathcal{O}_{k2}^{(1)} + \mathcal{V}_{k2}^{(T)} \mathcal{O}_{k1}^{(T)}$ to the vNRQCD Lagrangian with Wilson coefficients $\mathcal{V}_{k1}^{(1)}$ and $\mathcal{V}_{k2}^{(T)}$, respectively. The μ_S^ϵ factors in Eq. (41) are determined as in

sections II,III. In Eq. (41) the functions f_i are

$$\begin{aligned} f_0 &= \frac{\mathbf{p}' \cdot (\mathbf{q} - \mathbf{p})}{(\mathbf{q} - \mathbf{p})^4 (\mathbf{q} - \mathbf{p}')^2} + (\mathbf{p} \leftrightarrow \mathbf{p}'), & f_1 &= \frac{\mathbf{q} \cdot (\mathbf{q} - \mathbf{p})}{(\mathbf{q} - \mathbf{p})^4 (\mathbf{q} - \mathbf{p}')^2} + (\mathbf{p} \leftrightarrow \mathbf{p}'), \\ f_2 &= \frac{(\mathbf{q} - \mathbf{p}') \cdot (\mathbf{q} - \mathbf{p})}{(\mathbf{q} - \mathbf{p})^4 (\mathbf{q} - \mathbf{p}')^4} (\mathbf{q}^2 - \mathbf{p}'^2/2 - \mathbf{p}^2/2). \end{aligned} \quad (42)$$

If the finite sums over \mathbf{q} were carried out as integrals d^3q or d^nq with $n = d - 1 \rightarrow 3$ then the operators $\mathcal{O}_{ki}^{(1,T)}$ would reduce to $1/|\mathbf{k}|$ potentials. However, in general it is the operators in Eq. (41) which are the fundamental quantities as discussed in Sec. III. The counterterms required to cancel the divergences in the two-body ultrasoft graphs in Fig. 7a,b,c plus the corresponding soft divergences determined by the pull-up mechanism [17] are

$$\delta\mathcal{V}_{k1}^{(1)} = -\frac{2C_A C_1}{3\pi} \left[\frac{\alpha_s(\mu_U)}{\epsilon} - \frac{\alpha_s(\mu_S)}{\epsilon} \right], \quad \delta\mathcal{V}_{k2}^{(T)} = \frac{C_A(C_A + C_d)}{6\pi} \left[\frac{\alpha_s(\mu_U)}{\epsilon} - \frac{\alpha_s(\mu_S)}{\epsilon} \right]. \quad (43)$$

Next consider the order $\alpha^4 v^{-1}$ ultrasoft graphs. At this order there are two diagrams (shown in Figs. 8a,b) with ultrasoft gluons which contain divergences that are not canceled by counterterms from $\mathcal{V}_{2,r,k1,k2}$ [18]. A part of the UV divergences in Fig. 8b is canceled by a $\delta\mathcal{V}_{k1,k2}$ counterterm graph involving the function f_2 as shown in Fig. 8c. Similar to the graphs in Fig. 7 the remaining divergences are subtracted by operators with sums over \mathbf{q}, \mathbf{q}' as pictured in Fig. 7d. The required operators are

$$\begin{aligned} \mathcal{O}_{c1}^{(1)} &= -[\mu_S^{2\epsilon} \mathcal{V}_c^{(T)}]^3 \sum_{\mathbf{p}, \mathbf{p}', \mathbf{q}, \mathbf{q}'} (2h_0 - h_1) [\psi_{\mathbf{p}'}^\dagger \psi_{\mathbf{p}} \chi_{-\mathbf{p}'}^\dagger \chi_{-\mathbf{p}}], \\ \mathcal{O}_{c2}^{(T)} &= -[\mu_S^{2\epsilon} \mathcal{V}_c^{(T)}]^3 \sum_{\mathbf{p}, \mathbf{p}', \mathbf{q}, \mathbf{q}'} h_0 [\psi_{\mathbf{p}'}^\dagger T^A \psi_{\mathbf{p}} \chi_{-\mathbf{p}'}^\dagger \bar{T}^A \chi_{-\mathbf{p}}], \\ \mathcal{O}_{c3}^{(T)} &= -[\mu_S^{2\epsilon} \mathcal{V}_c^{(T)}]^3 \sum_{\mathbf{p}, \mathbf{p}', \mathbf{q}, \mathbf{q}'} h_1 [\psi_{\mathbf{p}'}^\dagger T^A \psi_{\mathbf{p}} \chi_{-\mathbf{p}'}^\dagger \bar{T}^A \chi_{-\mathbf{p}}], \end{aligned} \quad (44)$$

where $\mathcal{V}_{c1}^{(1)}, \mathcal{V}_{c2}^{(T)}, \mathcal{V}_{c3}^{(T)}$ are the corresponding Wilson coefficients that appear in the resulting contribution to the vNRQCD Lagrangian, $\Delta\mathcal{L}_p = \mathcal{V}_{c1}^{(1)} \mathcal{O}_{c1}^{(1)} + \mathcal{V}_{c2}^{(T)} \mathcal{O}_{c2}^{(T)} + \mathcal{V}_{c3}^{(T)} \mathcal{O}_{c3}^{(T)}$. The μ_S^ϵ factors in Eq. (44) are determined as discussed in sections II,III. The functions $h_{0,1}$ have the form

$$\begin{aligned} h_0 &= \frac{(\mathbf{q}' - \mathbf{p}') \cdot (\mathbf{q} - \mathbf{p})}{(\mathbf{q} - \mathbf{p})^4 (\mathbf{q} - \mathbf{q}')^2 (\mathbf{q}' - \mathbf{p}')^4}, \\ h_1 &= \frac{(\mathbf{q} - \mathbf{q}') \cdot (\mathbf{q} - \mathbf{p})}{(\mathbf{q} - \mathbf{p})^4 (\mathbf{q} - \mathbf{q}')^4 (\mathbf{q}' - \mathbf{p}')^2} + (\mathbf{p} \leftrightarrow \mathbf{p}', \mathbf{q} \leftrightarrow \mathbf{q}'). \end{aligned} \quad (45)$$

The counterterms needed to cancel the ultrasoft divergences in Figs. 8a,b,c plus the soft divergences determined by the pull-up [18] are

$$\begin{aligned} \delta\mathcal{V}_{c1}^{(1)} &= \frac{C_A C_1 (C_A + C_d)}{12\pi} \left[\frac{\alpha_s(\mu_U)}{\epsilon} - \frac{\alpha_s(\mu_S)}{\epsilon} \right], \\ \delta\mathcal{V}_{c2}^{(T)} &= \frac{4C_A C_1}{3\pi} \left[\frac{\alpha_s(\mu_U)}{\epsilon} - \frac{\alpha_s(\mu_S)}{\epsilon} \right], \\ \delta\mathcal{V}_{c3}^{(T)} &= \frac{2C_A}{3\pi} \left[C_1 + \frac{(C_A + C_d)^2}{32} \right] \left[\frac{\alpha_s(\mu_U)}{\epsilon} - \frac{\alpha_s(\mu_S)}{\epsilon} \right]. \end{aligned} \quad (46)$$

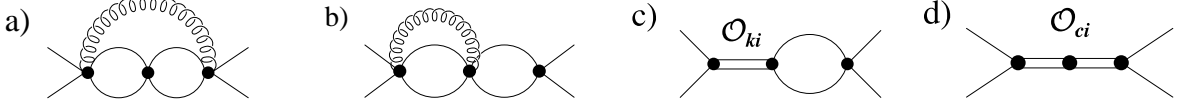


FIG. 8: Graphs for the renormalization of the operator which leads to the $1/\mathbf{k}^2$ potential.

From the counterterms in Eqs. (43) and (46) the vRGE gives the anomalous dimensions $[\gamma_{u2}(\nu) \equiv 2\alpha_s(m\nu^2) - \alpha_s(m\nu)]$

$$\begin{aligned} \nu \frac{\partial}{\partial \nu} \mathcal{V}_{k1}^{(1)} &= -\frac{4C_A C_1}{3\pi} \gamma_{u2}(\nu), & \nu \frac{\partial}{\partial \nu} \mathcal{V}_{k2}^{(T)} &= \frac{C_A(C_A + C_d)}{3\pi} \gamma_{u2}(\nu), \\ \nu \frac{\partial}{\partial \nu} \mathcal{V}_{c1}^{(1)} &= \frac{C_A C_1 (C_A + C_d)}{6\pi} \gamma_{u2}(\nu), & \nu \frac{\partial}{\partial \nu} \mathcal{V}_{c2}^{(T)} &= \frac{8C_A C_1}{3\pi} \gamma_{u2}(\nu), \\ \nu \frac{\partial}{\partial \nu} \mathcal{V}_{c3}^{(T)} &= \frac{4C_A}{3\pi} \left[C_1 + \frac{(C_A + C_d)^2}{32} \right] \gamma_{u2}(\nu). \end{aligned} \quad (47)$$

Note that possible soft graphs which could contribute to these anomalous dimensions are exactly canceled by $\mathcal{V}_c^{(T)}$ counterterms similar to the QED example in Sec. III. Using the boundary conditions $\mathcal{V}_{ki}^{(1,T)}(1) = \mathcal{V}_{ci}^{(1,T)}(1) = 0$ we find the solutions

$$\begin{aligned} \mathcal{V}_{k1}^{(1)}(\nu) &= \frac{8C_A C_1}{3\beta_0} \ln(w), & \mathcal{V}_{k2}^{(T)}(\nu) &= -\frac{2C_A(C_A + C_d)}{3\beta_0} \ln(w), \\ \mathcal{V}_{c1}^{(1)}(\nu) &= -\frac{C_A C_1 (C_A + C_d)}{3\beta_0} \ln(w), & \mathcal{V}_{c2}^{(T)}(\nu) &= -\frac{16C_A C_1}{3\beta_0} \ln(w), \\ \mathcal{V}_{c3}^{(T)}(\nu) &= -\frac{8C_A}{3\beta_0} \left[C_1 + \frac{(C_A + C_d)^2}{32} \right] \ln(w), \end{aligned} \quad (48)$$

where w is given in Eq. (35). These are our final results for the Wilson coefficients of the new operators in Eqs. (41) and (44). The corresponding color singlet channel coefficients are given by $\mathcal{V}^{(s)} = \mathcal{V}^{(1)} - C_F \mathcal{V}^{(T)}$ (where coefficients for color structures not shown in Eqs. (41) and (44) such as $\mathcal{V}_{k1}^{(T)}$ are zero at this order).

With the operators in Eqs. (41) and (44) all divergences in the usoft diagrams in Figs. 7a,b,c and 8a,b,c are canceled completely. Therefore, the corresponding contributions in the anomalous dimensions for the potential coefficients $\mathcal{V}_{k,c}^{(1,T)}$ in Eq. (6) obtained in Refs. [17, 18] should be removed. The only remaining divergences that must be canceled by $\mathcal{V}_{k,c}^{(1,T)}$ are from purely soft diagrams and are associated with the known running of the strong coupling α_s . Thus we find

$$\begin{aligned} \nu \frac{\partial}{\partial \nu} \mathcal{V}_k^{(T)}(\nu) &= -\frac{\beta_0}{8\pi} (7C_A - C_d) [\alpha_s(m\nu)]^3, & \nu \frac{\partial}{\partial \nu} \mathcal{V}_k^{(1)}(\nu) &= -\frac{\beta_0}{2\pi} C_1 [\alpha_s(m\nu)]^3, \\ \nu \frac{\partial}{\partial \nu} \mathcal{V}_c^{(T)}(\nu) &= -2 \left[\beta_0 \alpha_s^2(m\nu) + \beta_1 \frac{\alpha_s^3(m\nu)}{4\pi} + \beta_2 \frac{\alpha_s^4(m\nu)}{(4\pi)^2} \right], \end{aligned} \quad (49)$$

where $\beta_{0,1,2}$ are the coefficients of the QCD beta function (in the $\overline{\text{MS}}$ scheme for β_2). With the matching conditions at $\nu = 1$ [16] these equations give the solutions

$$\mathcal{V}_k^{(T)}(\nu) = \frac{(7C_A - C_d)}{8} \alpha_s^2(m\nu), \quad \mathcal{V}_k^{(1)}(\nu) = \frac{C_1}{2} \alpha_s^2(m\nu), \quad \mathcal{V}_c^{(T)}(\nu) = 4\pi \alpha_s^{[3]}(m\nu). \quad (50)$$

Here $\alpha_s^{[3]}(m\nu)$ is the QCD coupling with 3-loop running.

It must be noted that in general the operators \mathcal{O}_{kj} and \mathcal{O}_{cj} , are *not* directly related to the potentials $1/|\mathbf{k}|$ and $1/\mathbf{k}^2$ in Eq. (6). The reason is that the sums over \mathbf{q}, \mathbf{q}' must be regulated in the same way as sums over \mathbf{p}, \mathbf{p}' . This has important implications for the cancelation of subdivergences as discussed in Sec. III and therefore also affects renormalized matrix elements as we will discuss further in the next two sections. However, if we take *finite* matrix elements of the $1/|\mathbf{k}|$ and $1/\mathbf{k}^2$ potentials and operators \mathcal{O}_{kj} and \mathcal{O}_{cj} , then we can use $\sum_{\mathbf{q}} f_0 = \sum_{\mathbf{q}} f_1/3 = \sum_{\mathbf{q}} f_2 = 1/(16|\mathbf{k}|)$ and $\sum_{\mathbf{q}, \mathbf{q}'} h_0 = \sum_{\mathbf{q}, \mathbf{q}'} h_1/2 = 1/(64\pi^2\mathbf{k}^2)$. The result for the finite matrix element is then equivalent to the matrix element of effective $1/|\mathbf{k}|$ and $1/\mathbf{k}^2$ potentials with modified Wilson coefficients:

$$\begin{aligned}\mathcal{V}_{k,\text{eff}}^{(1)} &= \mathcal{V}_k^{(1)}(\nu) + 6\alpha_s^2(m\nu)\mathcal{V}_{k1}^{(1)}(\nu), & \mathcal{V}_{k,\text{eff}}^{(T)} &= \mathcal{V}_k^{(T)}(\nu) + 4\alpha_s^2(m\nu)\mathcal{V}_{k2}^{(T)}(\nu), \\ \mathcal{V}_{c,\text{eff}}^{(1)} &= \mathcal{V}_c^{(1)}(\nu), & \mathcal{V}_{c,\text{eff}}^{(T)} &= \mathcal{V}_c^{(T)}(\nu) + \pi\alpha_s^3(m\nu)\left[\mathcal{V}_{c2}^{(T)}(\nu) + 2\mathcal{V}_{c3}^{(T)}(\nu)\right].\end{aligned}\quad (51)$$

Substituting in the solutions in Eqs. (48) and (50) this gives the following effective color singlet coefficients

$$\begin{aligned}\mathcal{V}_{k,\text{eff}}^{(s)} &= \frac{C_F}{2}(C_F - 2C_A)\alpha_s^2(m\nu) + \frac{8C_FC_A(C_A + 2C_F)}{3\beta_0}\alpha_s^2(m\nu)\ln(w), \\ \mathcal{V}_{c,\text{eff}}^{(s)} &= -4\pi C_F\alpha_s^{[3]}(m\nu) + \frac{2\pi C_FC_A^3}{3\beta_0}\alpha_s^3(m\nu)\ln(w).\end{aligned}\quad (52)$$

We emphasize that these effective coefficients can only be used for finite matrix elements, and in this case they should be viewed simply as a shorthand way of accounting for insertions of the \mathcal{O}_{ki} and \mathcal{O}_{ci} operators and the $1/|\mathbf{k}|$ and $1/\mathbf{k}^2$ potentials. The results for these effective coefficients agree with the results for the coefficients of the $1/|\mathbf{k}|$ and $1/\mathbf{k}^2$ potentials in Refs. [21, 24] for scales $\mu < m\nu$ (pNRQCD), but only *if* we impose the scale correlation $\nu_{us} = m\nu^2$, and $1/r = m\nu$ as mentioned previously in Sec. V. Again, our results do not agree with Refs. [21, 24] for scales $m\nu < \mu < m$ (mNRQCD). Furthermore, except for finite matrix elements, our results disagree with Refs. [17, 18, 21, 24] since we have found that the anomalous dimensions are associated to a different set of operators which includes \mathcal{O}_{k1} , \mathcal{O}_{k2} , \mathcal{O}_{c1} , \mathcal{O}_{c2} , and \mathcal{O}_{c3} rather than just the $1/|\mathbf{k}|$ and $1/\mathbf{k}^2$ potentials. In general these operators contribute in a different way for matrix elements with divergences.

VII. RESULTS FOR THE PRODUCTION CURRENT

The leading order production currents in the effective theory are of order v^3 and produce a $q\bar{q}$ pair in a 3S_1 or 1S_0 state:

$$\mathbf{J}_{1,\mathbf{p}} = \psi_{\mathbf{p}}^\dagger \boldsymbol{\sigma}(i\sigma_2)\chi_{-\mathbf{p}}^*, \quad J_{0,\mathbf{p}} = \psi_{\mathbf{p}}^\dagger (i\sigma_2)\chi_{-\mathbf{p}}^*. \quad (53)$$

where $c_1(\nu)$ and $c_0(\nu)$ are the corresponding Wilson coefficients. The fields are evaluated at spacetime coordinate x . The two-loop matching for $c_1(1)$ and $c_0(1)$ were first considered in Refs. [32, 33], and are scheme dependent. With the potentials used here the matching onto $c_1(1)$ is known in the $\overline{\text{MS}}$ scheme at two-loop order [19, 20]. This matching condition is not affected by our new soft operators $\mathcal{O}_{2i}^{(2)}$ or the potential operators $\mathcal{O}_{ki,ci}$ since their Wilson coefficients vanish identically at the hard scale.

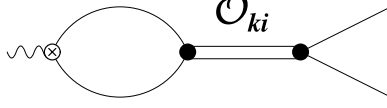


FIG. 9: Contribution to the anomalous dimension for the production current from $\mathcal{O}_{k1}^{(1)}$, $\mathcal{O}_{k2}^{(T)}$.

The currents in Eq. (53) receive a non-trivial NLL anomalous dimension from graphs starting at order $\alpha_s^2 v^0$ which were computed in Ref. [14]. However, this anomalous dimension is affected by our \mathcal{O}_{ki} operators which were not included there. The additional contribution is through the graph in Fig. 9 and we find the result

$$\begin{aligned} \gamma_{c_1}(\nu) = \nu \frac{\partial}{\partial \nu} \ln[c_1(\nu)] = & -\frac{\mathcal{V}_c^{(s)}(\nu)}{16\pi^2} \left[\frac{\mathcal{V}_c^{(s)}(\nu)}{4} + \mathcal{V}_2^{(s)}(\nu) + \mathcal{V}_r^{(s)}(\nu) + \mathbf{S}^2 \mathcal{V}_s^{(s)}(\nu) \right] \\ & + \frac{1}{2} \mathcal{V}_k^{(s)}(\nu) + \alpha_s^2(m\nu) [3\mathcal{V}_{k1}^{(s)}(\nu) + 2\mathcal{V}_{k2}^{(s)}(\nu)], \end{aligned} \quad (54)$$

where $\mathbf{S}^2 = 2$ for this spin-triplet coefficient. The anomalous dimension for the spin singlet coefficient c_0 is identical to $\gamma_{c_1}(\nu)$, but with $\mathbf{S}^2 = 0$. The last term in Eq. (54) which is proportional to $\alpha_s^2(m\nu)$ is the contribution from Fig. 9. However, it is easy to see from Eq. (51) that in this case the sum of the last two terms is simply equal to $V_{k,\text{eff}}^{(s)}(\nu)/2$ so that

$$\gamma_{c_1}(\nu) = -\frac{\mathcal{V}_c^{(s)}(\nu)}{16\pi^2} \left[\frac{\mathcal{V}_c^{(s)}(\nu)}{4} + \mathcal{V}_2^{(s)}(\nu) + \mathcal{V}_r^{(s)}(\nu) + \mathbf{S}^2 \mathcal{V}_s^{(s)}(\nu) \right] + \frac{1}{2} \mathcal{V}_{k,\text{eff}}^{(s)}(\nu). \quad (55)$$

To see how this comes about note that the counterterms for the graph involving the $1/|\mathbf{k}|$ potentials and the one in Fig. 9 are respectively

$$\begin{aligned} \delta c_1 &= \frac{1}{4\epsilon} \mathcal{V}_k^{(s)}(\nu), \\ \delta c_1 &= \frac{1}{8\epsilon} [6\mathcal{V}_{k1}^{(1)}(\nu) - 4C_F \mathcal{V}_{k2}^{(T)}(\nu)] \alpha_s^2(m\nu) = \frac{1}{8\epsilon} [\mathcal{V}_{k,\text{eff}}^{(s)}(\nu) - \mathcal{V}_k^{(s)}(\nu)]. \end{aligned} \quad (56)$$

However, the factor of two difference is made up for by the fact that there is an additional relative factor of two in determining the anomalous dimensions $\nu \partial/\partial \nu \mathcal{V}_k^{(s)} = -2\epsilon \mathcal{V}_k^{(s)} + \dots$, and $\nu \partial/\partial \nu [\alpha_s^2 \mathcal{V}_{ki}^{(s)}] = -4\epsilon [\alpha_s^2 \mathcal{V}_{ki}^{(s)}] + \dots$ in dimensional regularization (to be compared with $\mu \partial/\partial \mu \alpha_s = -2\epsilon \alpha_s + \dots$). This difference stems from the factors $\mu_s^{2\epsilon}$ and $\mu_s^{4\epsilon}$ in Eqs. (5) and (41), respectively. In the next section we will consider an example where the $\mathcal{V}_{k1,k2}$ coefficients do not come in the linear combination in $\mathcal{V}_{k,\text{eff}}$.

Solving Eq. (54) we find $[z = \alpha_s(m\nu)/\alpha_s(m), w = \alpha_s(m\nu^2)/\alpha_s(m\nu)]$

$$\begin{aligned} \ln \left[\frac{c_1(\nu)}{c_1(1)} \right] = & +a_2 \pi \alpha_s(m) (1-z) + a_3 \pi \alpha_s(m) \ln(z) \\ & +a_4 \pi \alpha_s(m) \left[1 - z^{1-13C_A/(6\beta_0)} \right] + a_5 \pi \alpha_s(m) \left[1 - z^{1-2C_A/\beta_0} \right] \\ & +a_0 \pi \alpha_s(m) \left[(z-1) - w^{-1} \ln(w) \right], \end{aligned} \quad (57)$$

where the coefficients a_4 and a_5 agree with Ref. [17]

$$a_4 = \frac{24C_F^2(11C_A-3\beta_0)(5C_A+8C_F)}{13C_A(6\beta_0-13C_A)^2}, \quad a_5 = \frac{C_F^2[C_A(15-14\mathbf{S}^2)+\beta_0(4\mathbf{S}^2-3)]}{6(\beta_0-2C_A)^2}, \quad (58)$$

where $\mathbf{S}^2 = 2$. The modifications to the running potentials appearing in Eq. (54) cause the remaining terms to differ

$$\begin{aligned}
a_2 &= \frac{C_F [C_A C_F (9C_A - 100C_F) - \beta_0 (26C_A^2 + 19C_A C_F - 32C_F^2)]}{26\beta_0^2 C_A}, \\
a_3 &= \frac{C_F^2}{\beta_0^2 (6\beta_0 - 13C_A)(\beta_0 - 2C_A)} \left\{ C_A^2 (9C_A - 100C_F) + \beta_0 C_A [74C_F + C_A (13\mathbf{S}^2 - 42)] \right. \\
&\quad \left. - 6\beta_0^2 [2C_F + C_A (\mathbf{S}^2 - 3)] \right\}, \\
a_0 &= -\frac{8C_F (C_A + C_F) (C_A + 2C_F)}{3\beta_0^2}. \tag{59}
\end{aligned}$$

For the solution for $c_0(\nu)$ one should substitute $\mathbf{S}^2 = 0$ in the a_i coefficients.

It is important to note that the anomalous dimension $\gamma_{c_1}(\nu)$ in Eqs. (54,55) arises from divergences in potential loop diagrams which must be computed with a dynamic fermion propagator $i/[E - \mathbf{p}^2/(2m)]$ [14]. In Ref. [17] it was shown that this anomalous dimension correctly reproduces the $\alpha_s^3 \ln^2 \alpha_s$ terms in the wavefunction at the origin first computed in Ref. [34].² For this to be the case it was necessary to include both soft and ultrasoft contributions to the running potentials on the right hand side of Eq. (54). As the scale for this anomalous dimension travels from m to mv it was necessary to simultaneously have the soft loop contributions vary from m to mv at the same rate, and have the ultrasoft loops vary from m to mv^2 . Furthermore, in the Appendix of Ref. [20] it was found that the relation $\mu_U = \mu_S^2/m$ is required for a consistent subtraction of subdivergences coming from ultrasoft and potential divergences in three-loop vertex diagrams that contribute to the NNLL anomalous dimension of the production currents. This shows that ultrasoft gluons are needed starting at the scale m . It also shows that it is necessary to simultaneously have divergent loops with ultrasoft, soft and potential momentum in the theory.

We believe that for dynamic quarks these facts are difficult to reconcile from the point of view of the mNRQCD–pNRQCD formalism. The existence of mNRQCD–pNRQCD seems to depend crucially on there being a non-trivial stage of matching that occurs at a scale $\mu \simeq mv \simeq 1/r$ where soft gluons are integrated out, while the above results seem to indicate that such an intermediate matching scale does not exist in general. This does not mean that results obtained with the mNRQCD–pNRQCD formalism are necessarily wrong for dynamic quarks, but seems to imply that they may require some reinterpretation.

In Ref. [25] a procedure was developed which reproduces the anomalous dimension in Eq. (55) in the framework of the mNRQCD–pNRQCD formalism. In our opinion, the procedure suggested in Ref. [25] contradicts some features of mNRQCD–pNRQCD upon which other results seem to rely. In particular, in Ref. [25] it was proposed to a) demand a correlation between the energy and momentum scales but only for the c_1 computation, b) transport the $1/r$ matching scale back up to m by hand so that ultrasoft gluons exist for all scales $\mu < m$, and c) allow couplings associated with soft loops to become unfrozen and run down again from m . With this construction the potentials used in Ref. [25] on the RHS of Eq. (55) agree with ours, so the solution in Eq. (54) agrees with the one in Ref. [25]

² This result is not changed by our results here since the coefficient of the first log in the resummed $\mathcal{V}_j^{(s)}$ coefficients is the same as in Ref. [17] and $\int d\nu/\nu \ln \nu = (\ln^2 \nu)/2$.

setting $\nu_p = m\nu$. For this to be the case it was crucial that it was the combination $\mathcal{V}_{k,\text{eff}}^{(s)}$ that appeared in Eq. (55), and that the corresponding contributions in Ref. [25] were treated in the same way as they are predicted to be treated by vNRQCD. We agree with Ref. [25] that static quarks can be used to simplify certain calculations, in particular those with soft loops. However, our conclusion is then that mNRQCD does not exist by itself as a physical theory that can be used to make predictions with dynamic quarks.

Our results for the running of $c_1(\nu)$ and the $\mathcal{V}_j^{(s)}(\nu)$ have implications for the case where Λ_{QCD} becomes comparable to mv^2 . Take $mv^2 \sim \Lambda_{\text{QCD}}$ and consider decreasing ν from $\nu = 1$. As the cutoff on momentum transfers and quark momenta, $m\nu$, gets close to mv , the μ_U scale in the ultrasoft $\alpha_s(\mu_U)$ couplings is approaching the scale Λ_{QCD} . Since ultrasoft gluons renormalize the potentials these effects are tied together as soon as ultrasoft gluons first start to renormalize operators. Thus, as $m\nu$ gets close to mv , a scale affecting the coefficients $\mathcal{V}_j(\nu)$ of the potentials approaches Λ_{QCD} .³ Considering one ultrasoft gluon the affected potentials include the spin-independent $1/m^2$ potentials, and effective $1/|\mathbf{k}|$ and $1/\mathbf{k}^2$ potentials (or more properly the \mathcal{O}_{ci} and \mathcal{O}_{ki} operators). Furthermore, due to the correlation between E and $\mathbf{p}^2/(2m)$ for the heavy quarks, non-perturbative effects at the energy scale could lead to non-perturbative effects for the momenta. One conclusion is that for $mv^2 \sim \Lambda_{\text{QCD}}$ we can become sensitive to non-perturbative scales through the potentials even for cutoffs near the momentum transfer $m\nu \gg \Lambda_{\text{QCD}}$. This seems quite problematic for perturbatively matching onto the potentials at a scale $\mu = m\nu$ for dynamic quarks. However, this does not affect the matching for static quarks as done with the mNRQCD-pNRQCD formalism in Ref. [13]. For $b\bar{b}$ states with dynamic quarks and $mv^2 \sim \Lambda_{\text{QCD}}$, this might also imply that non-perturbative effects have a larger influence than one usually infers.

VIII. TOP PRODUCTION AT THRESHOLD AND QUARKONIUM ENERGIES

The results for the order v^{-1} , v^0 and v^1 QCD potentials and the new operators \mathcal{O}_{ki} and \mathcal{O}_{ci} presented in the previous sections affect the results for the NLL and NNLL top threshold e^+e^- cross section that were given in Refs. [19, 20] and the NNLL quarkonium energies given in Ref. [18]. Except for the handling of the \mathcal{O}_{ki} and $1/|\mathbf{k}|$ potentials discussed below, the changes all involve simply substituting in the coefficients $\mathcal{V}_2^{(s)}$ and $\mathcal{V}_r^{(s)}$ given in Eq. (38) and replacing $\mathcal{V}_c^{(s)}$ by the $\mathcal{V}_{c,\text{eff}}^{(s)}$ given in Eq. (52).

The modified results for the coefficients of the order v^1 spin-independent potentials, $\mathcal{V}_2^{(s)}$ and $\mathcal{V}_r^{(s)}$, and the production current, c_1 , affect the results only trivially through the modified running of the coefficients. They do not lead to any change in the analytic form of the NLL and NNLL corrections to the current correlator \mathcal{A}_1 . For the corrections caused by the v^{-1} (Coulomb) potential and the operators \mathcal{O}_{ci} it is sufficient to consider the effective Coulomb potential coefficient in Eq. (52) because the corresponding matrix elements do not lead to UV divergences which affect the cross section. Thus, in the results presented in Ref. [19, 20] one simply has to replace $\mathcal{V}_c^{(s)} \rightarrow \mathcal{V}_{c,\text{eff}}^{(s)}$ and there is no other change. In Table. I we compare results for the coefficients at $\nu = 0.15$ and $\nu = 0.3$. The changes are smaller for

³ The evolution towards the scale Λ_{QCD} due to ultrasoft gluons can still be computed perturbatively. This is very much like the fact that the evolution for the region $\Lambda_{\text{QCD}} < \mu < m_c$ in $B \rightarrow D$ decays can be computed perturbatively [35]. One must just be careful not to evolve too close to the scale Λ_{QCD} .

| | $\mathcal{V}_r^{(s)}(\nu)$ | $\mathcal{V}_2^{(s)}(\nu)$ | $\pi^2 \mathcal{V}_{k,\text{eff}}^{(s)}(\nu)$ | $\mathcal{V}_{c,\text{eff}}^{(s)}(\nu)$ | $c_1(\nu)/c_1(1)$ |
|-----------------------------|----------------------------|----------------------------|---|---|-------------------|
| matching ($\nu = 1$) | -1.81 | 0 | -0.357 | -1.800 | 1.000 |
| old results ($\nu = .3$) | -1.72 | 0.361 | -0.256 | -2.153 | 1.034 |
| new results ($\nu = .3$) | -1.68 | 0.359 | -0.238 | -2.153 | 1.034 |
| old results ($\nu = .15$) | -1.51 | 0.616 | -0.043 | -2.423 | 1.046 |
| new results ($\nu = .15$) | -1.39 | 0.609 | 0.016 | -2.425 | 1.044 |

TABLE I: Comparison of the numerical change to the Wilson coefficients for $t\bar{t}$ ($m_t = 175 \text{ GeV}$). The old results show the coefficients used in Ref. [20], while the new results use the coefficients from Sects. V and VI. For the first three columns and the fourth column we use 1-loop running for α_s , while the last column uses 3-loop running. The coefficient $\mathcal{V}_s^{(s)}(\nu)$ is unchanged from the result in Ref. [15] and is not shown.

the larger value of ν as expected. For $\nu = 0.15$ we see that the changes in $\mathcal{V}_2^{(s)}$, $\mathcal{V}_c^{(s)}$ and $c_1(\nu)$ are still very small (1.1%, 0.08% and 0.2%, respectively), while $\mathcal{V}_r^{(s)}$ changes by a more moderate amount (8%). For completeness $V_{k,\text{eff}}^{(s)}$ is also shown, even though it is not just this combination of coefficients that appears in the cross section. Since $V_{k,\text{eff}}^{(s)}(\nu)$ has a zero near $\nu \simeq 0.15$ the relative change for this value of ν is quite large. A more relevant measure is the suppression of $\mathcal{V}_{k,\text{eff}}^{(s)}$ at $\nu \simeq 0.15$ compared to at $\nu = 1$, which is observed in both results. The effect of these changes on the cross section are discussed later in this section.

The new results for the v^0 potentials and the operators \mathcal{O}_{ki} lead to analytic changes in the NNLL corrections to the current correlator \mathcal{A}_1 because the corresponding matrix elements are UV divergent and the n -dependent contributions that arise from summing the potential indices in the operators \mathcal{O}_{ki} in dimensional regularization lead to modifications of the UV-finite terms. With dimensional regularization the full n -dependent ($n = d - 1$) expression for the potential that appears in the Schrödinger equation from the operators \mathcal{O}_{ki} (and \mathcal{O}_{ci}) is given in App. B. Altogether, there are now three different types of corrections to the current correlator δG^k , δG^{k1} , and δG^{k2} , that are needed to account for the corrections originating from the singlet $1/|\mathbf{k}|$ potential and the operators \mathcal{O}_{k1} and \mathcal{O}_{k2} , respectively. Using $\overline{\text{MS}}$ we find

$$\begin{aligned}
\delta G^{k1}(a, v, m, \nu) &= -\frac{3m^2}{4\pi a} \left\{ i v - a \left[\ln \left(\frac{-i v}{\nu} \right) - \frac{17}{12} + \ln 2 + \gamma_E + \Psi \left(1 - \frac{i a}{2 v} \right) \right] \right\}^2 \\
&\quad + \frac{3m^2}{4\pi a} \left[-v^2 + \frac{a^2}{16} \left(\frac{1}{\epsilon^2} - \frac{11}{3\epsilon} - \frac{89}{9} \right) \right], \\
\delta G^{k2}(a, v, m, \nu) &= -\frac{m^2}{2\pi a} \left\{ i v - a \left[\ln \left(\frac{-i v}{\nu} \right) - \frac{21}{16} + \ln 2 + \gamma_E + \Psi \left(1 - \frac{i a}{2 v} \right) \right] \right\}^2 \\
&\quad + \frac{m^2}{2\pi a} \left[-v^2 + \frac{a^2}{16} \left(\frac{1}{\epsilon^2} - \frac{13}{4\epsilon} - \frac{175}{16} \right) \right], \tag{60}
\end{aligned}$$

In deriving these equations we have included the counterterm generated by renormalizing the \mathbf{J}_1 current at NLL order in Eq. (56). These counterterm graphs are sufficient to cancel all subdivergences. The remaining overall divergences shown in Eq. (60) are canceled

by counterterms for the current correlator. For comparison the term δG^k from the $1/|\mathbf{k}|$ potential which was given in Ref. [20] is:

$$\delta G^k(a, v, m, \nu) = -\frac{m^2}{8\pi a} \left\{ i v - a \left[\ln \left(\frac{-i v}{\nu} \right) - 2 + 2 \ln 2 + \gamma_E + \Psi \left(1 - \frac{i a}{2 v} \right) \right] \right\}^2 + \frac{m^2}{8\pi a} \left[-v^2 + \frac{a^2}{4} \left(\frac{1}{3\epsilon^2} - \frac{2}{\epsilon} \left(1 - \frac{2}{3} \ln 2 \right) + \frac{4}{3} - 8 \ln 2 + \frac{8}{3} \ln^2 2 + \frac{\pi^2}{9} \right) \right], \quad (61)$$

where this expression is also renormalized in the way described above. Since the δG^{ki} are not proportional to δG^k , it is in general *not* the linear combination of coefficients defined in $\mathcal{V}_{k,\text{eff}}^{(s)}$ in Eq. (52) that appears in the cross section. The NNLL vector correlator

$$\mathcal{A}_1(v, m, \nu) = i \sum_{\mathbf{p}, \mathbf{p}'} \int d^4 x e^{i\hat{q} \cdot x} \left\langle 0 \left| T \mathbf{J}_{1,\mathbf{p}}(x) \mathbf{J}_{1,\mathbf{p}'}^\dagger(0) \right| 0 \right\rangle \quad (62)$$

can be expressed in terms of the renormalized Greens functions as

$$\begin{aligned} \mathcal{A}_1 = 6 N_c & \left[G^c(a', v, m, \nu) + \left(\mathcal{V}_2^{(s)}(\nu) + 2\mathcal{V}_s^{(s)}(\nu) \right) \delta G^\delta(a, v, m, \nu) + \mathcal{V}_r^{(s)}(\nu) \delta G^r(a, v, m, \nu) \right. \\ & + \mathcal{V}_k^{(s)}(\nu) \delta G^k(a, v, m, \nu) + \alpha_s^2(m\nu) \mathcal{V}_{k1}^{(1)}(\nu) \delta G^{k1}(a, v, m, \nu) \\ & \left. - C_F \alpha_s^2(m\nu) \mathcal{V}_{k2}^{(T)}(\nu) \delta G^{k2}(a, v, m, \nu) + \delta G^{\text{kin}}(a, v, m, \nu) \right], \quad (63) \end{aligned}$$

$$a = -\frac{1}{4\pi} \mathcal{V}_c^{(s)}(\nu), \quad a' = -\frac{1}{4\pi} \mathcal{V}_{c,\text{eff}}^{(s)}(\nu), \quad (64)$$

where $\hat{q} = (\sqrt{s} - 2m, \mathbf{0})$, m is the top quark pole mass, $v = (\sqrt{s} - 2m + i\Gamma_t)/m)^{1/2}$, and the expressions for $G^c(a, v, m, \nu)$, and $\delta G^{\delta,r,\text{kin}}(a, v, m, \nu)$ are given in Ref. [20]. The combination $\text{Im}[c_1^2(\nu)\mathcal{A}_1]$ then appears in R^v , which is the normalized vector current induced cross section. From analyzing Eq. (63) we see that while the coefficients of some functions are proportional to $\mathcal{V}_{k,\text{eff}}^{(s)}$, the coefficients of other terms are not. For instance we have terms such as $\mathcal{V}_{k,\text{eff}}^{(s)} \Psi^2(z)$, however the combination $(34\mathcal{V}_{k1}^{(s)} + 21\mathcal{V}_{k2}^{(s)})\Psi(z)$ also appears. Therefore, in general the effective $1/|\mathbf{k}|$ potential is not sufficient and the individual expressions for the $\mathcal{V}_{k,k1,k2}(\nu)$ contributions are required.

Our results for the $\mathcal{V}_j^{(s)}$ coefficients also numerically affect the NNLL relation between the 1S mass and the pole mass, which is needed to switch to the 1S mass scheme [36]. This relation is obtained from the 3S_1 ground state solution of the Schrödinger equation and is given in Eq. (46) of Ref. [20]. The modifications caused by the order v^1 potentials are again trivial, and only the coefficients $\mathcal{V}_r^{(s)}$ and $\mathcal{V}_2^{(s)}$ are changed. For the NNLL energy levels the matrix elements of the \mathcal{O}_{ci} and \mathcal{O}_{ki} operators do not cause additional UV divergences, so the effect of these operators can be implemented simply by replacing $\mathcal{V}_c^{(s)}$ and $\mathcal{V}_k^{(s)}$ in Ref. [20] by $\mathcal{V}_{c,\text{eff}}^{(s)}$ and $\mathcal{V}_{k,\text{eff}}^{(s)}$ respectively. Thus, the additional correction to the current correlator \mathcal{A}_1 caused by switching to the 1S mass scheme has the same functional form as before

$$\delta \mathcal{A}_1(v, M^{1S}, \nu) = -6 N_c \frac{\Delta_m^{\text{NNLL}}}{v} \frac{d}{dv} G^0(a, v, M^{1S}, \nu) \quad (65)$$

$$\Delta_m^{\text{NNLL}} = -\frac{a^2}{8} \mathcal{V}_{k,\text{eff}}^{(s)} - \frac{a^3}{8\pi} \left(\frac{\mathcal{V}_2^{(s)}}{2} + \mathcal{V}_s^{(s)} + \frac{3\mathcal{V}_r^{(s)}}{8} \right) + \frac{5}{128} a^4,$$

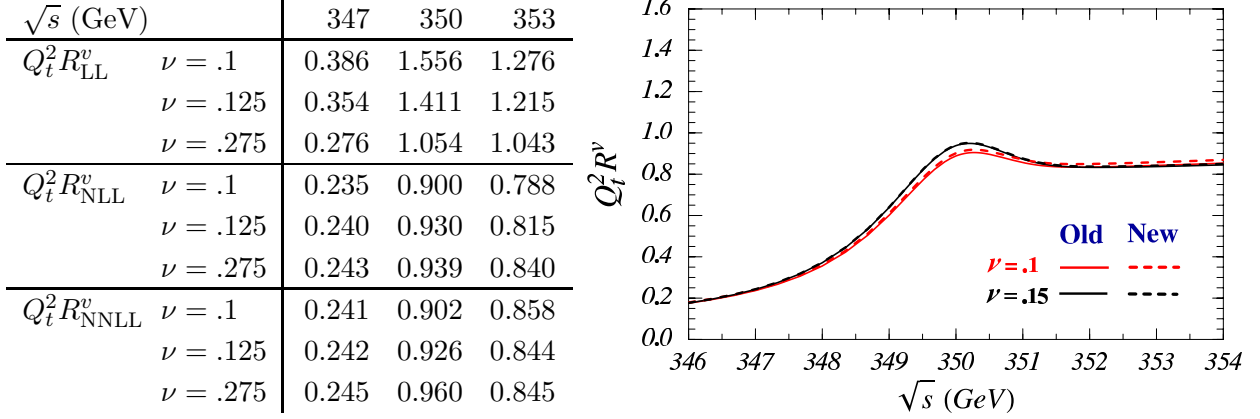


FIG. 10: Updated numerical values of $Q_t R^v$ in the 1S mass scheme. Also shown is a figure comparing the old NNLL results from Ref. [20] (solid curves) and our new results (dashed curves) for two values of ν (red $\nu = 0.1$, and black $\nu = 0.15$). Near the peak it is easy to see that the scale uncertainty is several times larger than the difference between the old and new results.

where G^0 is the LL zero-distance Greens function of the Schrödinger equation given in Eq. (34) of Ref. [20]. The formula for the heavy quarkonium spectrum for arbitrary quantum numbers is also affected by simply replacing coefficients in Eq. (40) of Ref. [18] just as in the expression for the 3S_1 ground state energy described above.

Next we turn to how our results numerically affect the vector-current-induced top threshold cross section R^v at NLL and NNLL order. We will see that the change is quite small and well within the error estimate of Ref. [20]. Note that the axial-vector cross section R^a does not receive any modifications as it depends only on the LL value of $\mathcal{V}_c^{(s)}$ at this order.

In Fig. 10 we have displayed our updated values of $Q_t^2 R^v$ in the 1S mass scheme as a function of the c.m. energy \sqrt{s} for $M^{1S} = 175$ GeV, $\alpha_s(m_Z) = 0.118$ and $\Gamma_t = 1.43$ GeV, and taking four-loop running for α_s with $n_f = 5$ active massless quark flavors. The numerical methods used to evaluate G_c were described in Ref. [37]. We also show a figure comparing our NNLL results to those in Ref. [20] for $\nu = 0.1$ and $\nu = 0.15$. The relative deviation is quite small and essentially independent of the c.m. energy at NLL and NNLL order. Note that this is obvious for the NLL cross section, because at this order only the coefficient c_1 is affected by the new results. For $\sqrt{s} = 350$ GeV the relative deviation amounts to (2.2%, 1.0%, 1.0%, 0.6%, 0.3%, 0.1%) at NLL order and to (1.5%, 0.6%, 0.2%, 0.01%, 0.1%, 0.1%) at NNLL order for $\nu = (0.1, 0.125, 0.15, 0.2, 0.275, 0.4)$. This is well within the relative uncertainty of $\pm 3\%$ for the normalization of $Q_t^2 R^v$ at NNLL order which we estimated in Ref. [20].

In Fig. 11a we have displayed $Q_t^2 R^v$ up to NNLL order. The curves show the LL (dotted glue lines), NLL (dashed green lines) and NNLL (solid red lines) cross section for $\nu = 0.1, 0.125, 0.2$ and 0.4 , where at LL order lower curves correspond to larger values of ν . The conclusions drawn from these results are the same as in Ref. [20]. Thus, compared to earlier NNLO (fixed order) results [38] the variation of the normalization of the NNLL cross section with ν is considerably reduced. Equally important, the sum of all NNLL corrections is about an order of magnitude smaller than the size of the NNLO corrections [38], and agrees well with the predictions at NLL order. This indicates that the expansion is converging.

In Figs. 11b, c and d we have displayed separately, the contributions to $Q_t^2 R^v$ coming from G^c (dashed lines), from the sum of $\delta G^{k,1,k,2}$ (dotted lines) and the sum of $\delta G^{\delta,r,\text{kin},1S}$

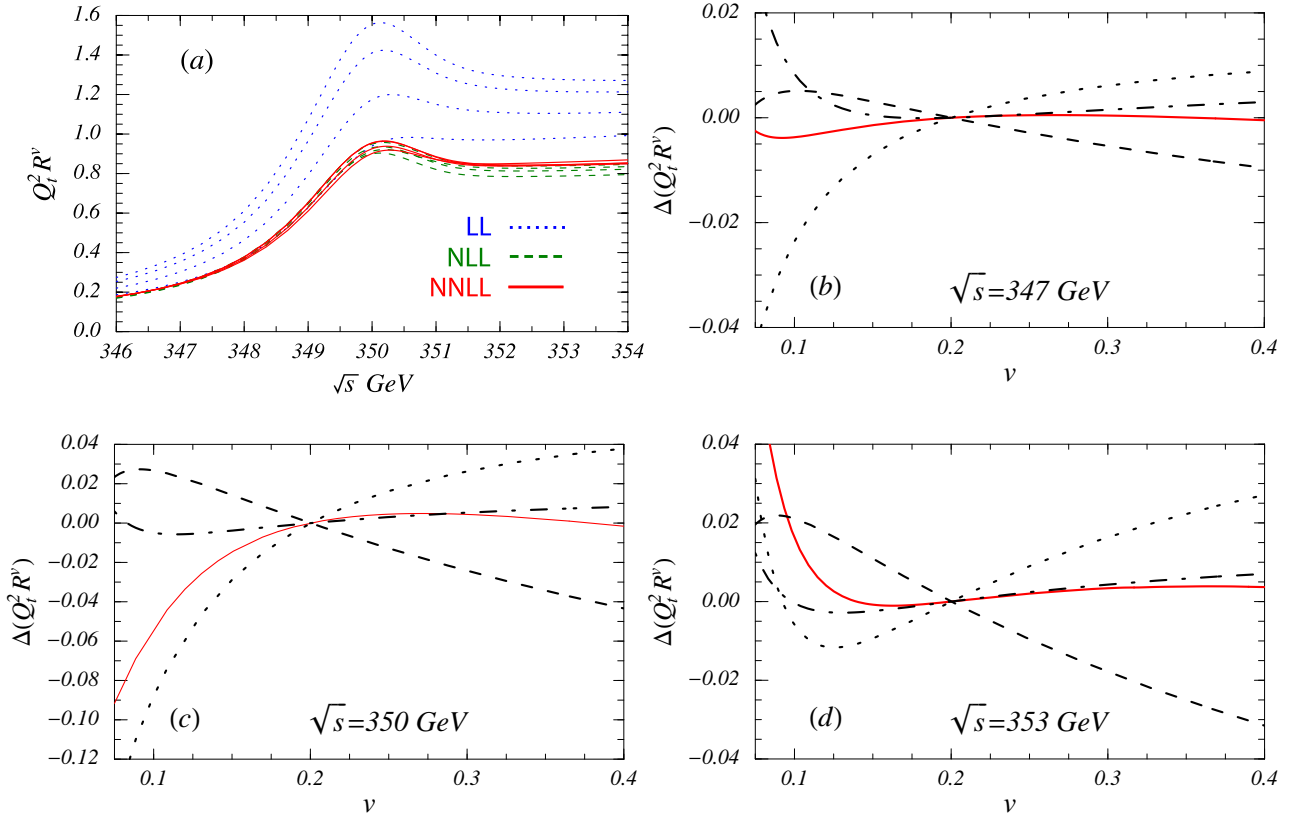


FIG. 11: Panel a) shows the NNLL results for $Q_t^2 R^v$ with $M^{1S} = 175$ GeV at LL (dotted lines), NLL (dashed lines) and NNLL (solid lines) order. For each order four curves are plotted for $\nu = 0.1, 0.125, 0.2$ and 0.4 . Panels b)-d) show the relative scale dependence of various NNLL contributions to $Q_t^2 R^v$ for different c.m. energies. The contributions are divided into those from G^c (dashed lines), the sum off $\delta G^{k,k1,k2}$ (dotted line), and the sum of $\delta G^{\delta,r,\text{kin},1S}$ (dot-dashed lines) while the solid (red) lines denote the sum of these terms, $Q_t R^v$. Note that the plots have different scales for the y-axes.

(dot-dashed lines) as a function of ν for $\sqrt{s} = 347, 350$ and 353 GeV. In general we find for $\nu \gtrsim 0.15$ that the ν -variation of the contributions from G^c and from the sum of $\delta G^{k,k1,k2}$ cancel to a large extent, whereas the contributions from $\delta G^{\delta,r,\text{kin},1S}$ are almost ν -independent. On the other hand, for values of $\nu < 0.15$ and energies around and above the peak position the ν -variation is dominated by the contributions from $\delta G^{k,k1,k2}$, which rapidly increase in size for decreasing ν , whereas the contributions from G^c and $\delta G^{\delta,r,\text{kin},1S}$ are small. The behavior of these results are in agreement with our previous results in Refs. [19, 20] and shows that the modified results for the potentials and the effects of the new operators \mathcal{O}_{ci} and \mathcal{O}_{ki} lead only to small numerical changes while the essential properties remain unchanged. To be more specific, making a conservative estimate by using the value 0.1 as the lower bound for the velocity scaling parameter [20] to determine the remaining theoretical uncertainties of the NNLL renormalization group improved cross section we find

$$\frac{\delta\sigma_{t\bar{t}}}{\sigma_{t\bar{t}}} = \pm 3\%. \quad (66)$$

This agrees with our earlier estimate in Ref. [20] and is an order of magnitude smaller than the uncertainties associated to fixed order NNLO QCD computations [38]. In particular, the conclusions that we have drawn in Ref. [20] concerning the theoretical uncertainties in extractions of α_s , the top Yukawa coupling and the total top width from a threshold scan at a future linear collider remain unchanged and are comparable to the expected experimental uncertainties [39].

IX. CONCLUSION

In this paper we have reconsidered the renormalization group improvement of Wilson coefficients in NRQCD in light of two new observations about the structure of ultrasoft renormalization of operators.

We first showed that the ultrasoft renormalization of operators with soft gluons can induce through mixing operators $\mathcal{O}_{2i}^{(2)}$ whose Wilson coefficients vanish at the matching scale. Taking four quark matrix elements of these operators then causes a renormalization of the spin-independent $1/m^2$ potentials. Using the notation for the $1/m^2$ potential in Eq. (6) this analysis affects the running of the coefficients $\mathcal{V}_2(\nu)$ and $\mathcal{V}_r(\nu)$ in QCD. Our results are different from Ref. [15] where these additional operators were not included. We also compared our results to those in the mNRQCD–pNRQCD approach in Ref. [24]. Our results do not agree with the running of 4-quark operators in mNRQCD because we find that the renormalization from ultrasoft gluons is present for all scales $\mu < m$. We did find agreement with the pNRQCD results if we imposed a correlation between the mNRQCD–pNRQCD matching and renormalization scales, $\nu_{us} = m\nu^2$ and $1/r = m\nu$. This agreement is encouraging, however our correlation requirement may have implications for the NRQCD analysis of the case $m\nu^2 \sim \Lambda_{\text{QCD}}$, as discussed in Sec. VII and mentioned below.

Second we performed an analysis of graphs containing mixed ultrasoft and potential loops and gave a new procedure for subtracting divergences in these graphs. In particular we find that ultrasoft gluons renormalize the operators \mathcal{O}_{ki} and \mathcal{O}_{ci} displayed in Eqs. (41) and (44), rather than the $1/|\mathbf{k}|$ and $1/\mathbf{k}^2$ potentials. Because of this our results differ from those in Refs. [17, 18, 21, 24]. In certain situations with finite matrix elements it is possible to make use of effective $1/|\mathbf{k}|$ and $1/\mathbf{k}^2$ potentials with modified Wilson coefficients. However in general this is not the case. An example of the former are predictions for the NNLL perturbative quarkonium energy levels, while an example of the latter are current correlators which give the $e^+e^- \rightarrow t\bar{t}$ cross sections as discussed in Sec. VIII.

We also considered the implications of the modified running for the evolution of the production current (Sec. VII) and for predictions for the $t\bar{t}$ cross section at NNLL order. For the cross section the change from the results in Ref. [19, 20] is very small, being $\lesssim 1\%$ for the physically motivated values $\nu > 0.15$. If we include a larger more conservative range of scale variations then the change is still small becoming 1.5% at $\nu = 0.1$. Since the uncertainty assigned to predictions in Ref. [20] was $\pm 3\%$, all analyses and conclusions for the cross section are unchanged. In particular, there is still a large improvement in the convergence of the perturbation theory over not summing the logarithms, and we can assign a conservative overall uncertainty of $\pm 3\%$ to the NNLL cross section predictions which is much smaller than the uncertainty found at NNLO [38].

Our results for the running have implications for cases where Λ_{QCD} becomes comparable to $m\nu^2$. Essentially, since ultrasoft gluons renormalize spin-independent potential operators these potentials become sensitive to the scale Λ_{QCD} at an earlier stage than might otherwise

be thought. The list of affected potentials includes the spin-independent $1/m^2$ potentials and the \mathcal{O}_{ci} and \mathcal{O}_{ki} operators (which give effects often attributed to the $1/|\mathbf{k}|$ and $1/\mathbf{k}^2$ potentials). Due to the correlation for $mv^2 \sim \Lambda_{\text{QCD}}$ we are sensitive to non-perturbative scales through the potentials even though the momentum transfer $mv \gg \Lambda_{\text{QCD}}$. This seems problematic for perturbatively matching onto the potentials at a scale $\mu = mv$ for dynamic quarks, because at this scale the coefficients of the potentials are already blowing up.

Acknowledgments

We would like to thank A. Manohar for many useful discussions and gratefully acknowledge communication with A. Penin on the nature of the $n_f \alpha_s^5 \ln^2 \alpha$ corrections to the $1/\mathbf{k}^2$ potential. We also thank A. Manohar and I. Rothstein for comments on the manuscript. We thank the Benasque Center of Science, where part of this work was carried out, and I.S. would like to thank the Max-Planck-Institut in Munich for their hospitality while this work was completed. This work was supported in part by the Department of Energy under the grant DE-FG03-00-ER-41132.

APPENDIX A: SUMMARY OF STRUCTURES FOR SIX FIELD OPERATORS

The structures appearing in the QCD operators $\mathcal{O}_{2\varphi}^{(0)}$, $\mathcal{O}_{2A}^{(0)}$, and $\mathcal{O}_{2c}^{(0)}$ include

$$\begin{aligned}
\Gamma_{\varphi}^{(0)} &= \left[T^A T^B \frac{(2q^0 \gamma^0 + \mathbf{k} \cdot \boldsymbol{\gamma})}{\mathbf{k}^2 + 2\mathbf{k} \cdot \mathbf{q}} + T^B T^A \frac{(2q^0 \gamma^0 - \mathbf{k} \cdot \boldsymbol{\gamma})}{\mathbf{k}^2 - 2\mathbf{k} \cdot \mathbf{q}} \right] \left(Z_0^{(0)} \right)^2, \\
\Gamma_{\varphi,\psi}^{(0)} &= T^A, \quad \Gamma_{\varphi,\chi}^{(0)} = \bar{T}^B \\
\Gamma_{A,\mu\nu}^{(0),CD} &= -\frac{1}{2} f^{AEC} f^{BED} \left[U_{\mu\sigma}^{(0)}(q, \mathbf{p}, \mathbf{p}') (U^{(0)})_{\nu}{}^{\sigma}(-q, -\mathbf{p}, -\mathbf{p}') \right] \frac{1}{\mathbf{k}^2 + 2\mathbf{k} \cdot \mathbf{q}} \\
&\quad - \frac{1}{2} f^{AED} f^{BEC} \left[U_{\mu\sigma}^{(0)}(-q, \mathbf{p}, \mathbf{p}') (U^{(0)})_{\nu}{}^{\sigma}(q, -\mathbf{p}, -\mathbf{p}') \right] \frac{1}{\mathbf{k}^2 - 2\mathbf{k} \cdot \mathbf{q}}, \\
\Gamma_{A,\psi}^{(0)} &= T^A, \quad \Gamma_{A,\chi}^{(0)} = \bar{T}^B \\
\Gamma_c^{(0),CD} &= \left[\frac{f^{AEC} f^{BED}}{\mathbf{k}^2 + 2\mathbf{k} \cdot \mathbf{q}} + \frac{f^{AED} f^{BEC}}{\mathbf{k}^2 - 2\mathbf{k} \cdot \mathbf{q}} \right] \left(Y_0^{(0)} \right)^2, \\
\Gamma_{c,\psi}^{(0)} &= T^A, \quad \Gamma_{c,\chi}^{(0)} = \bar{T}^B \tag{A1}
\end{aligned}$$

where the $U_{\mu\nu}^{(0)}$, $Z_0^{(0)}$, and $Y_0^{(0)}$ coefficients can be found in Ref. [15]. We have also made use of color contractions of these structures including

$$\begin{aligned}
\Gamma_{\varphi}^{(0),(1)} &= \Gamma_{\varphi}^{(0),(T)} = \frac{1}{2} \left[\frac{(2q^0 \gamma^0 + \mathbf{k} \cdot \boldsymbol{\gamma})}{\mathbf{k}^2 + 2\mathbf{k} \cdot \mathbf{q}} + \frac{(2q^0 \gamma^0 - \mathbf{k} \cdot \boldsymbol{\gamma})}{\mathbf{k}^2 - 2\mathbf{k} \cdot \mathbf{q}} \right] \left(Z_0^{(0)} \right)^2, \\
\Gamma_{\phi,\psi}^{(0),(T)} &= T^A, \quad \Gamma_{\phi,\chi}^{(0),(T)} = \bar{T}^A, \quad \Gamma_{\phi,\psi}^{(0),(1)} = 1, \quad \Gamma_{\phi,\chi}^{(0),(1)} = 1, \\
\Gamma_{A,\mu\nu}^{(0),(T)} &= \Gamma_{A,\mu\nu}^{(0),(1)} = -\frac{C_A}{2} \left\{ \left[U_{\mu\sigma}^{(0)}(q, \mathbf{p}, \mathbf{p}') (U^{(0)})_{\nu}{}^{\sigma}(-q, -\mathbf{p}, -\mathbf{p}') \right] \frac{1}{\mathbf{k}^2 + 2\mathbf{k} \cdot \mathbf{q}} \right. \\
&\quad \left. + \left[U_{\mu\sigma}^{(0)}(-q, \mathbf{p}, \mathbf{p}') (U^{(0)})_{\nu}{}^{\sigma}(q, -\mathbf{p}, -\mathbf{p}') \right] \frac{1}{\mathbf{k}^2 - 2\mathbf{k} \cdot \mathbf{q}} \right\}, \\
\Gamma_{A,\psi}^{(0),(T)} &= T^A, \quad \Gamma_{A,\chi}^{(0),(T)} = \bar{T}^A, \quad \Gamma_{A,\psi}^{(0),(1)} = 1, \quad \Gamma_{A,\chi}^{(0),(1)} = 1, \\
\Gamma_{c,\psi}^{(0),(T)} &= \Gamma_{c,\psi}^{(0),(1)} = C_A \left[\frac{1}{\mathbf{k}^2 + 2\mathbf{k} \cdot \mathbf{q}} + \frac{1}{\mathbf{k}^2 - 2\mathbf{k} \cdot \mathbf{q}} \right] \left(Y_0^{(0)} \right)^2, \\
\Gamma_{c,\psi}^{(0),(T)} &= T^A, \quad \Gamma_{c,\chi}^{(0),(T)} = \bar{T}^A, \quad \Gamma_{c,\psi}^{(0),(1)} = 1, \quad \Gamma_{c,\chi}^{(0),(1)} = 1. \tag{A2}
\end{aligned}$$

APPENDIX B: FORM OF POTENTIALS IN THE SCHRÖDINGER EQUATION

When the $1/|\mathbf{k}|$ potential and the operators \mathcal{O}_{k1} and \mathcal{O}_{k2} are included in the Schrödinger equation in dimensional regularization the form of the potential is

$$V_k^{\text{Schr.}}(\mathbf{p}, \mathbf{q}) = \frac{\pi^2 \mu_S^{2\epsilon}}{m|\mathbf{k}|} \mathcal{V}_k^{(s)}(\nu) + \frac{\pi^2 \mu_S^{4\epsilon}}{m(\mathbf{k}^2)^{2-\frac{n}{2}}} \alpha_s^2(m\nu) \mathcal{V}_{k1}^{(1)}(\nu) \left[8(n^2 - 5n - 12) f(1, 1) \right] \\ - \frac{\pi^2 \mu_S^{4\epsilon}}{m(\mathbf{k}^2)^{2-\frac{n}{2}}} C_F \alpha_s^2(m\nu) \mathcal{V}_{k2}^{(T)}(\nu) \left[4(n^2 - 3n + 8) f(1, 1) \right], \quad (\text{B1})$$

while for the $1/\mathbf{k}^2$ potential and the operators \mathcal{O}_{c1} , \mathcal{O}_{c2} , and \mathcal{O}_{c3} the potential is

$$V_c^{\text{Schr.}}(\mathbf{p}, \mathbf{q}) = \frac{\mu_S^{2\epsilon}}{\mathbf{k}^2} \mathcal{V}_c^{(s)}(\nu) + \frac{64\pi^3 \mu_S^{6\epsilon}}{(\mathbf{k}^2)^{4-n}} C_F \alpha_s(m\nu)^3 \left(\frac{1}{2} \mathcal{V}_{c2}^{(T)} + \mathcal{V}_{c3}^{(T)} \right) \\ \times \left[(4-n) f(1, 2) f\left(3 - \frac{n}{2}, 1\right) \right], \quad (\text{B2})$$

where

$$f(a, b) = \frac{\Gamma(a + b - \frac{n}{2}) \Gamma(\frac{n}{2} - a) \Gamma(\frac{n}{2} - b)}{\Gamma(a) \Gamma(b) \Gamma(n - a - b) (4\pi)^{\frac{n}{2}}}. \quad (\text{B3})$$

In Eq. (B2) the operator \mathcal{O}_{c1} gives a vanishing contribution. Note that the functions $1/(\mathbf{k}^2)^{2-n/2}$ and $1/(\mathbf{k}^2)^{4-n}$ are *not* the d-dimensional Fourier transform of a $1/r^2$ or $1/r$ potential. Also note that in another regularization scheme such as with a cutoff, the potentials in Eqs. (B1) and (B2) would take a different functional form, however the momentum dependence of the \mathcal{V}_k , $\mathcal{V}_{k1,k2}$, \mathcal{V}_c , and $\mathcal{V}_{c2,c3}$ terms would still differ from each other.

-
- [1] A. H. Hoang, arXiv:hep-ph/0204299; N. Brambilla, arXiv:hep-ph/0012026; I. Z. Rothstein, arXiv:hep-ph/9911276; M. Beneke, arXiv:hep-ph/9703429.
 - [2] W.E. Caswell and G.P. Lepage, Phys. Lett. **167B**, 437 (1986).
 - [3] G.T. Bodwin, E. Braaten and G.P. Lepage, Phys. Rev. **D51**, 1125 (1995), *ibid.* **D55**, 5853 (1997).
 - [4] P. Labelle, Phys. Rev. **D58**, 093013 (1998) [arXiv:hep-ph/9608491].
 - [5] M. Luke and A.V. Manohar, Phys. Rev. **D55**, 4129 (1997) [arXiv:hep-ph/9610534].
 - [6] B. Grinstein and I.Z. Rothstein, Phys. Rev. **D57**, 78 (1998) [arXiv:hep-ph/9703298].
 - [7] M. Luke and M.J. Savage, Phys. Rev. **D57**, 413 (1998) [arXiv:hep-ph/9707313].
 - [8] A. Pineda and J. Soto, Nucl. Phys. Proc. Suppl. **64**, 428 (1998) [arXiv:hep-ph/9707481].
 - [9] A.V. Manohar, Phys. Rev. **D56**, 230 (1997) [arXiv:hep-ph/9701294].
 - [10] M. Beneke and V.A. Smirnov, Nucl. Phys. **B522**, 321 (1998) [arXiv:hep-ph/9711391].
 - [11] H.W. Griesshammer, Phys. Rev. **D58**, 094027 (1998). [arXiv:hep-ph/9712467]. Nucl. Phys. B **579**, 313 (2000) [arXiv:hep-ph/9810235].
 - [12] A. Pineda and J. Soto, Phys. Rev. **D58**, 114011 (1998) [arXiv:hep-ph/9802365].
 - [13] N. Brambilla, A. Pineda, J. Soto and A. Vairo, Phys. Lett. **B470**, 215 (1999) [arXiv:hep-ph/9910238]; Nucl. Phys. **B566**, 275 (2000) [arXiv:hep-ph/9907240].

- [14] M. Luke, A. Manohar and I. Rothstein, Phys. Rev. **D61**, 074025 (2000) [arXiv:hep-ph/9910209].
- [15] A.V. Manohar and I.W. Stewart, Phys. Rev. D **62**, 014033 (2000) [arXiv:hep-ph/9912226].
- [16] A.V. Manohar and I.W. Stewart, Phys. Rev. **D62**, 074015 (2000) [arXiv:hep-ph/0003032].
- [17] A.V. Manohar and I.W. Stewart, Phys. Rev. **D63**, 54004 (2001). [arXiv:hep-ph/0003107].
- [18] A.H. Hoang, A.V. Manohar and I.W. Stewart, Phys. Rev. D **64**, 014033 (2001) [arXiv:hep-ph/0102257].
- [19] A. H. Hoang, A. V. Manohar, I. W. Stewart and T. Teubner, Phys. Rev. Lett. **86**, 1951 (2001) [arXiv:hep-ph/0011254].
- [20] A. H. Hoang, A. V. Manohar, I. W. Stewart and T. Teubner, Phys. Rev. D **65**, 014014 (2002) [arXiv:hep-ph/0107144].
- [21] A. Pineda and J. Soto, Phys. Lett. **B495**, 323 (2000) [arXiv:hep-ph/0007197].
- [22] A.V. Manohar and I.W. Stewart, Phys. Rev. Lett. **85**, 2248 (2000) [arXiv:hep-ph/0004018].
- [23] A.V. Manohar, J. Soto, and I.W. Stewart, Phys. Lett. **B486**, 400 (2000) [arXiv:hep-ph/0006096].
- [24] A. Pineda, Phys. Rev. D **65**, 074007 (2002) [arXiv:hep-ph/0109117].
- [25] A. Pineda, arXiv:hep-ph/0110216.
- [26] A. Pineda, arXiv:hep-ph/0204213.
- [27] A. Pineda, private communication.
- [28] K. Pachucki, Phys. Rev. **A53**, 2092 (1996).
- [29] C. Bauer and A. V. Manohar, Phys. Rev. D **57**, 337 (1998); E. Eichten and B. Hill, Phys. Lett. **B243**, 427 (1990); A.F. Falk, B. Grinstein and M.E. Luke, Nucl. Phys. **B357**, 185 (1991); B. Blok, J.G. Körner, D. Pirjol and J.C. Rojas, Nucl. Phys. **B496**, 358 (1997).
- [30] P. Labelle, Ph. D. thesis, Cornell University, 1994 (unpublished); K. Melnikov and A.S. Yelkhovsky, Phys. Lett. **B458**, 143 (1999).
- [31] Y. Chen, Y. Kuang and R. J. Oakes, Phys. Rev. **D52**, 264 (1995) [arXiv:hep-ph/9406287].
- [32] A. H. Hoang, Phys. Rev. **D56**, 7276 (1997) [arXiv:hep-ph/9703404]. A. Czarnecki and K. Melnikov, Phys. Rev. Lett. **80**, 2531 (1998) [arXiv:hep-ph/9712222]. M. Beneke, A. Signer and V. A. Smirnov, Phys. Rev. Lett. **80**, 2535 (1998) [arXiv:hep-ph/9712302].
- [33] A. Czarnecki and K. Melnikov, Phys. Rev. D **65**, 051501 (2002) [arXiv:hep-ph/0108233].
- [34] B. A. Kniehl and A. A. Penin, Nucl. Phys. **B577**, 197 (2000). [arXiv:hep-ph/9911414].
- [35] A. F. Falk, H. Georgi, B. Grinstein and M. B. Wise, Nucl. Phys. B **343**, 1 (1990).
- [36] A. H. Hoang, Z. Ligeti and A. V. Manohar, Phys. Rev. Lett. **82**, 277 (1999), Phys. Rev. D **59**, 074017 (1999); A. H. Hoang and T. Teubner, Phys. Rev. D **60**, 114027 (1999).
- [37] M. Jezabek, J. H. Kuhn and T. Teubner, Z. Phys. C **56** (1992) 653. T. Teubner, diploma thesis, University of Karlsruhe, 1992, unpublished; R. Harlander, diploma thesis, University of Karlsruhe, 1995, unpublished.
- [38] A. H. Hoang *et al.*, in Eur. Phys. J. direct **C3**, 1 (2000) [arXiv:hep-ph/0001286].
- [39] M. Martinez and R. Miquel, arXiv:hep-ph/0207315.